



Contents lists available at ScienceDirect

## Journal of the Mechanics and Physics of Solids

journal homepage: [www.elsevier.com/locate/jmps](http://www.elsevier.com/locate/jmps)

## Phase boundaries as agents of structural change in macromolecules

Ritwik Raj, Prashant K. Purohit \*

Department of Mechanical Engineering and Applied Mechanics, University of Pennsylvania, Philadelphia, PA 19104, USA

## ARTICLE INFO

## Article history:

Received 3 February 2011

Received in revised form

24 June 2011

Accepted 10 July 2011

Available online 20 July 2011

## Keywords:

Phase transformation

Biological material

Rod-like molecules

Finite differences

Polymeric material

## ABSTRACT

We model long rod-like molecules, such as DNA and coiled-coil proteins, as one-dimensional continua with a multi-well stored energy function. These molecules suffer a structural change in response to large forces, characterized by highly typical force-extension behavior. We assume that the structural change proceeds via a moving folded/unfolded interface, or phase boundary, that represents a jump in strain and is governed by the Abeyaratne–Knowles theory of phase transitions. We solve the governing equations using a finite difference method with moving nodes to represent phase boundaries. Our model can reproduce the experimental observations on the overstretching transition in DNA and coiled-coils and makes predictions for the speed at which the interface moves. We employ different types of kinetic relations to describe the mobility of the interface and show that this leads to different classes of experimentally observed force-extension curves. We make connections with several existing theories, experiments and simulation studies, thus demonstrating the effectiveness of the phase transitions-based approach in a biological setting.

© 2011 Elsevier Ltd. All rights reserved.

## 1. Introduction

The schematically simple Molecular Force Probe experiments have shed a great deal of light on the behavior of the macromolecules under the application of a point force. Single molecule mechanics experiments are performed in an AFM, magnetic tweezers or optical tweezers (Fig. 1). A molecule is held between rigid and semi-rigid supports in a fluid flow. The molecule is then stretched out by moving one of the supports, maintaining either a constant pulling velocity or a constant force. The result of these experiments is a force-extension curve of the individual molecule. The high degree of reproducibility of these curves makes them a suitable window to interpret how these molecules behave under simple tension.

Several macromolecules exhibit evidence of structural change at high forces. In the work presented in this paper, we have focused on the behavior of DNA under axial stretching. At 65 pN, the molecule undergoes a structural transition, the mechanism of which has still not been resolved completely. However, certain facts about this transition are indubitable. Around 65 pN, the force-extension curve changes suddenly from a sharply rising curve to a nearly flat plateau. The extension continues to increase for a very little increase in the force until the molecule has reached about 1.7 times its original contour length (Cluzel et al., 1996; Smith et al., 1996). At this point, the curve switches to another sharply rising curve, and further stretching eventually breaks the molecule. This transition is called an overstretching transition. It is accompanied by absorption of energy as the bonds holding the DNA in its native state are broken. There may also be a subsequent re-forming of bonds different from the ones just broken as is the case when  $\alpha$ -helical intermediate filaments are stretched leading to the formation of  $\beta$ -sheets after the unraveling of the  $\alpha$ -helices (Qin et al., 2009). We will not address the exact details of these changes in this paper.

\* Corresponding author. Tel.: +1 215 898 3870.

E-mail address: [purohit@seas.upenn.edu](mailto:purohit@seas.upenn.edu) (P.K. Purohit).

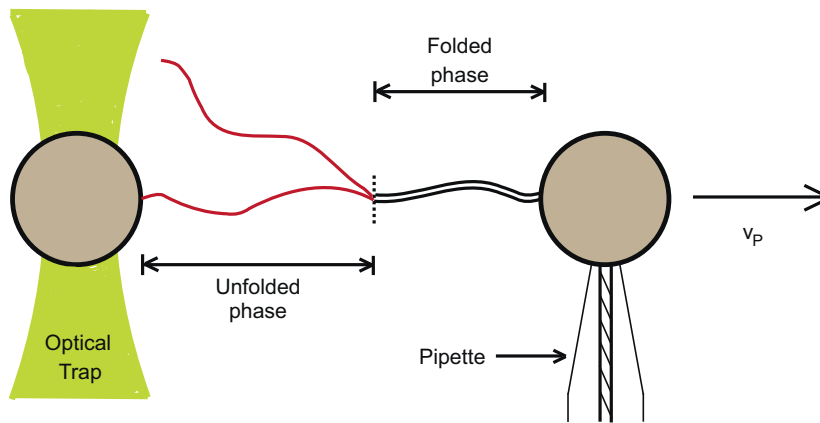


Fig. 1. Schematic diagram of the experimental apparatus.

It has been demonstrated that the rising parts of this curve can be fitted well with worm-like chain relations and two pairs of contour and persistence lengths. Both the mechanisms of the transition, as well as the intermediate states involved, have been vigorously debated over the past decade. At the center of the debate is the nature of the bonding between the two strands as the molecule gradually unfolds under the applied force. Various theories have claimed that this is due to the conversion of B-DNA to a unique intermediate state called S-DNA. Other studies have attempted to characterize the transition as a force-induced melting of double stranded DNA to single stranded DNA. These theories have their respective merits and there is experimental evidence in support of each (Rief et al., 1999; Rouzina and Bloomfield, 2001; Williams et al., 2002; Williams and Rouzina, 2002).

It is important to point out here that this type of plateau unfolding behavior is not unique to DNA. Many coiled-coil proteins are not only similar to DNA in structure (in that they are double helical), but also extremely similar in their response to forces. Plateaus like those seen in DNA have been observed in proteins like myosin II (Schwaiger et al., 2002) and desmin (Kreplak et al., 2008). This common feature of the response to tensile force in structures separated by two orders of magnitude in length and force is intriguing. Intermediate filaments, which are a category of structural proteins, share structural features of coiled-coils. Their importance is great in the study of mechanical properties of cells as they are capable of large, reversible deformations which have similar mechanisms to those in smaller proteins such as the myosin coiled-coil. Therefore, any results for smaller proteins hold considerable value in understanding structural properties of cells and their underlying intermediate filament networks.

### 1.1. Significance and approach of this work

In the body of literature devoted to this subject, there have been theories that incorporate the three distinct parts of the force-extension curve for DNA (Storm and Nelson, 2003; Chakrabarti and Levine, 2005). However, the rate dependence of the transition has not been fully addressed. There have been models proposed, that have shed light on the cooperative nature of the transition. These models have employed the concept of this structural change as being a phase transition and yielded results about the thermodynamics of the process. There have also been models that build upon the Arrhenius rate of reaction model. However, they involve fitting parameters which are largely arbitrary and do not yield further insights (Best et al., 2008; Rief et al., 1998). Also, until very recently, there was no visual evidence regarding how this transition progresses through the molecule. However, recently van Mameren et al. (2009) have demonstrated for the first time that interfaces exist in an unfolding DNA molecule during overstretching. Prior to this, Qin et al. (2009) had also demonstrated the existence of interfaces between folded and unfolded regions during atomistic level simulations for unfolding of a vimentin (a type of intermediate filament) dimer. In the work presented herewith, we have proposed a mechanism for this structural transition based on the motion of the interfaces through the molecule.

We have modeled the unfolding transition in DNA as a phase transition between two metastable phases, namely, the folded and the unfolded configurations. The DNA molecule in its native or folded state, also called B-DNA, has been modeled as a one-dimensional continuum with a constitutive law given by the worm-like chain relation (Marko and Siggia, 1995; Odijk, 1995). The unfolding has been assumed to proceed via a folded/unfolded front that moves along the molecule. The motion of this front or interface is governed by the Abeyaratne–Knowles theory of phase transitions (Abeyaratne and Knowles, 1993, 2006). This theory has been used with great success in studying phase transitions in bulk materials. In particular, the theory builds upon earlier work by Eshelby (1956, 1970) and Truskinovsky (1982, 1985), among others. In such cases, the motion of the interface is three-dimensional. However, we work with the advantage that the experiments under consideration are one-dimensional.

The key components of this model are the constitutive laws for the two phases and the kinetic relation, which relates the velocity of the interface to the thermodynamic driving force across it. This interface is technically best described as a discontinuity, and associated with this discontinuity are jump conditions and a thermodynamic driving force. The driving force is an important concept in classical phase transition theory, and it has been shown to have remarkable relevance in the current paradigm. We have derived expressions for all these quantities and also shown that only certain theoretical motions of the interface are practically possible depending on whether or not they satisfy the second law of thermodynamics. The nucleation criterion, which is the condition for the discontinuity to be nucleated, is also accounted for, in a simple manner.

Several kinetic relations have been used and they have captured a variety of the different motifs observed in the force-extension curves of not only DNA, but other macromolecules as well. The model is able to predict the speed at which the interface would have to move, while capturing with exactness, the force-extension profile. Recent experimental results have provided strong support for the assumption that the unfolding process proceeds via the motion of an interface. Even though the default setting is the one containing only one interface, multiple interfaces can also be generated. The model also reproduces well, the stretching and relaxation results for DNA in its untransformed state.

Calculations and predictions for energy dissipation during unfolding have also been presented. Circumstances for which the transition can be considered quasistatic have been elaborated upon. This work goes beyond existing literature in modeling the motion of the interface in non-equilibrium situations as well. In implementing this approach, we have used a minimum of arbitrary fitting parameters, choosing to use measured physical parameters as far as possible. The properties of the interface are central to the model and we have been able to demonstrate the effect of boundary conditions, especially the pulling velocity, on the motion of the interface.

## 2. Kinematics and balance laws

The kinematics of this problem follow the general framework derived for strings by Purohit and Bhattacharya (2003). In this paper, the authors consider a string that occupies the interval  $(0, L_c)$  in the reference configuration. This string may be located anywhere in three-dimensional space. The particle velocity, the stretch and the tangent to the string are allowed to have a finite number of jumps, but the deformation of the string is required to be continuous. In the problem considered in this paper, the molecule is always at high strain in the conditions of interest. Therefore, we assume that the deformation of the molecule is only in one direction, i.e. along its length. In fact, the problem at hand is similar to the bars considered in the development of the Abeyaratne–Knowles theory. We use the general framework to derive the kinematics for a rod-like molecule in one spatial dimension, and characterized by the scalar  $s$ , which is the reference configuration variable. We shall refer to  $s$  as the arc length position of a material point along the molecule. Since all vectors of interest have the same direction, these quantities will be treated as scalars with the understanding that the positive unit vector for them is along the length of the molecule, pointing from  $s=0$  to  $L_c$ .

In its most general form, this model treats a polymer as a purely one-dimensional continuum. The polymer is assumed to be placed in a fluid which can have a variable velocity along the length of the molecule, which causes a drag force. For the purpose of this fluid drag computation, the molecule is assumed to resemble a rod (Fig. 2). Also, while not strictly inextensible, the molecule is assumed to be such that the distance between any two monomers on the polymer backbone remains constant, irrespective of the force applied. The molecule exists at very low forces, in a very convoluted ball-like shape. The application of force has the effect of straightening out the polymer, but not extending its structure. Also, in the situations modeled in this work, there is assumed to be no twist in any part of the molecule. Therefore, the only type of deformation that this molecule can undergo is bending. This feature manifests itself as a worm-like chain constitutive law for the tensile behavior of the one-dimensional continuum. This law is a result of considering the effect of thermal fluctuations on the molecule. Thermal fluctuations are extremely prominent at the length scales we are considering and are responsible for the mechanical properties of the polymer. Increasing the extension may be interpreted as decreasing the number of configurations available to the molecule. The resultant reduction in the entropy makes it a non-spontaneous process and work must be done in order to drive it forward.

We now derive rigorously the kinematic framework of our system. The position of the particle  $s$  at time  $t$  is  $z(s, t)$ . The particle velocity is  $\partial z / \partial t$  or  $\dot{z}$ . The position- and time-dependent stretch  $|\partial z / \partial s|$  is denoted by  $\lambda$ . A single discontinuity is considered at  $s = x(t)$ .  $s > x(t)$  is termed as the  $+$  side and  $s < x(t)$  as the  $-$  side in the neighborhood of the discontinuity. For any quantity  $\phi$ , the jump  $\phi(s^+, t) - \phi(s^-, t)$  is denoted by  $[[\phi]]$ . Continuity of deformation implies  $[[z]] = 0$ .

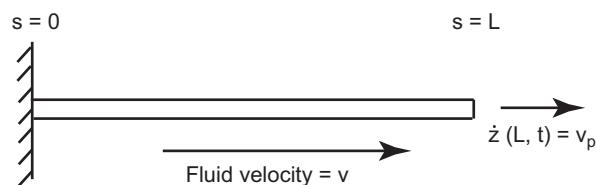


Fig. 2. Schematic diagram of a molecule modeled as a slender rod, with one fixed end and a constant velocity at the other end.

Differentiation with respect to time yields the kinematic jump condition:

$$\dot{\chi}[[\lambda]] + [[\dot{\chi}]] = 0. \tag{1}$$

The following relations have been used frequently in writing this relation and others in the text:

$$\phi(s_2) - \phi(s_1) = \int_{s_1}^{s_2} \frac{\partial \phi}{\partial s} ds + [[\phi]] \tag{2}$$

and

$$\frac{d}{dt} \int_{s_1}^{s_2} \phi ds = \int_{s_1}^{s_2} \dot{\phi} ds - \dot{\chi} [[\phi]]. \tag{3}$$

The balance of linear momentum for a portion of the molecule in the interval  $(s_1, s_2)$  in the reference configuration may be written as

$$\frac{d}{dt} \int_{s_1}^{s_2} \rho \dot{z} ds = f(s_2, t) - f(s_1, t) + \int_{s_1}^{s_2} b ds, \tag{4}$$

where  $\rho$  denotes the mass per unit length of the molecule in the reference configuration,  $f = f(s, t)$  denotes the force acting at material point  $s$  in the deformed configuration at time  $t$ , and  $b = b(s, t)$  denotes a distributed load per unit length at  $s$ . In our problem, the inertia force is negligible in comparison to the other forces involved. Thus, in the derivation that follows, we assume the density  $\rho$  to be zero. The distributed force  $b(s, t)$  in this case is a fluid drag force that is exerted on the molecule by the fluid surrounding it. This force is given by

$$b(s, t) = f_{drag}(s, t) = -d_w \left[ \frac{\partial z}{\partial t}(s, t) - v \right], \tag{5}$$

where  $d_w$  is the effective drag coefficient and  $v$  is the velocity of the surrounding fluid, which is assumed to flow only along the molecule. Hence, there is only axial drag and no drag normal to the molecule.  $d_w$  is estimated by results proposed by [Brennen and Winet \(1977\)](#) for slender bodies in low Reynolds' number flow. The objective of slender-body theory is to take advantage of the slenderness in order to achieve simplifications in obtaining approximate solutions for the flow around such bodies. The underlying principle of this theory is that solutions to many complex flows may be constructed by superposition of fundamental singularities around the object. For mathematically simple bodies such as spheroids in mathematically simple flow fields (uniform flow, shear flow, quadratic flow, extensional flow, etc.) exact solutions are obtained. Their expression for the axial drag coefficient is

$$d_w = \frac{2\pi\mu}{\log\left(\frac{2l}{a}\right) + c}, \tag{6}$$

where  $\mu$  is the fluid viscosity,  $2l$  is the length of the body,  $a$  is the radius of gyration of the body and  $c$  is a constant that depends upon the shape of the body. The value of  $c$  depends on the axial variation of the radius of the cylinder. A uniform axial cylinder took a value of  $c = \ln 2 - \frac{3}{2} = -0.807$ . Hence, the effective equation for momentum balance is

$$f(s_2, t) - f(s_1, t) - \int_{s_1}^{s_2} d_w \left[ \frac{\partial z}{\partial t}(s, t) - v \right] ds = 0. \tag{7}$$

If there are no discontinuities, we can localize (7) to get

$$\frac{\partial f}{\partial s} = d_w \left( \frac{\partial z}{\partial t} - v \right). \tag{8}$$

In case there is a discontinuity within the interval  $(s_1, s_2)$ , the appropriate jump condition is found by applying (2) and (3) to (7):

$$[[f]] = 0. \tag{9}$$

The balance of angular momentum consists of term-by-term cross products with the displacement vector. Since all vectors are collinear, all these products reduce to zero, and the balance of angular momentum yields no information.

An expression for the balance of mechanical power may be derived by taking the product of (8) with  $\dot{z}$ , which when integrated from  $s_1$  to  $s_2$  yields:

$$\int_{s_1}^{s_2} \frac{\partial f}{\partial s} \dot{z} ds = \int_{s_1}^{s_2} d_w (\dot{z} - v) \dot{z} ds, \tag{10}$$

which may be written as

$$\int_{s_1}^{s_2} \left[ \frac{\partial}{\partial s} (f\dot{z}) - f \frac{\partial \dot{z}}{\partial s} \right] ds = d_w \int_{s_1}^{s_2} |\dot{z}|^2 ds - d_w \int_{s_1}^{s_2} v \dot{z} ds. \tag{11}$$

Using (2) and (3), the above equation becomes

$$f\dot{\lambda}|_{s_1}^{s_2} - [f\dot{\lambda}] - \int_{s_1}^{s_2} f \frac{\partial \dot{\lambda}}{\partial s} ds = d_w \int_{s_1}^{s_2} |\dot{\lambda}|^2 ds - d_w \int_{s_1}^{s_2} v\dot{\lambda} ds. \quad (12)$$

Using the identity  $[(\mathbf{a} \cdot \mathbf{b})] = \langle \mathbf{a} \rangle \cdot [(\mathbf{b})] + \langle \mathbf{b} \rangle \cdot [(\mathbf{a})]$ , this can be further simplified to

$$f\dot{\lambda}|_{s_1}^{s_2} - f[|\dot{\lambda}|] - \int_{s_1}^{s_2} f \dot{\lambda} ds = d_w \int_{s_1}^{s_2} |\dot{\lambda}|^2 ds - d_w \int_{s_1}^{s_2} v\dot{\lambda} ds, \quad (13)$$

where we have also used the force jump condition (9). Further, substituting from the kinematic jump condition (1), we get

$$f\dot{\lambda}|_{s_1}^{s_2} + f\dot{\lambda}[|\lambda|] - \int_{s_1}^{s_2} f \dot{\lambda} ds = d_w \int_{s_1}^{s_2} |\dot{\lambda}|^2 ds - d_w v \int_{s_1}^{s_2} \dot{\lambda} ds. \quad (14)$$

The balance of energy for the molecule between  $s_1$  and  $s_2$  requires

$$\frac{d}{dt} \int_{s_1}^{s_2} \left( w + \frac{1}{2} \rho |\dot{\lambda}|^2 \right) ds = -q|_{s_1}^{s_2} + f\dot{\lambda}|_{s_1}^{s_2} - \int_{s_1}^{s_2} d_w (\dot{\lambda} - v)\dot{\lambda} ds, \quad (15)$$

where  $w = w(s, t)$  is the internal energy per unit length and  $q = q(s, t)$  is the heat flow rate in the tangential direction at a material point  $s$  at time  $t$ . An isothermal setting is assumed so there is no exchange of heat between the molecule and the bath in which it is placed. We note that in the absence of this assumption, though physically justified, the problem would have to be formulated in terms of a master equation. Continuing with our analysis, we see that in the absence of inertia, the above equation reduces to

$$\frac{d}{dt} \int_{s_1}^{s_2} w ds = f\dot{\lambda}|_{s_1}^{s_2} - \int_{s_1}^{s_2} d_w (\dot{\lambda} - v)\dot{\lambda} ds - q|_{s_1}^{s_2}. \quad (16)$$

Assuming a single discontinuity at  $s = x(t)$ , and using (14), we rewrite the above equation as

$$\frac{d}{dt} \int_{s_1}^{s_2} w ds = -f\dot{\lambda}[|\lambda|] + \int_{s_1}^{s_2} \left( f\dot{\lambda} - \frac{\partial q}{\partial s} \right) ds - [q]. \quad (17)$$

Using (3), this reduces to

$$\int_{s_1}^{s_2} \dot{w} ds - \dot{\lambda}[|w|] = -f\dot{\lambda}[|\lambda|] + \int_{s_1}^{s_2} \left( f\dot{\lambda} - \frac{\partial q}{\partial s} \right) ds - [q], \quad (18)$$

or

$$\int_{s_1}^{s_2} \left( \dot{w} - f\dot{\lambda} + \frac{\partial q}{\partial s} \right) ds = \dot{\lambda}([|w|] - f[|\lambda|]) - [q]. \quad (19)$$

Localizing this equation away from  $s = x(t)$ , we obtain the differential form of the balance of the energy:

$$\dot{w} = f\dot{\lambda} - \frac{\partial q}{\partial s}. \quad (20)$$

Localizing it to a discontinuity at  $s = x(t)$ , we get

$$\dot{\lambda}([|w|] - f[|\lambda|]) = [q]. \quad (21)$$

We now consider the entropy inequality. For the region of interest, this can be written as

$$\frac{d}{dt} \int_{s_1}^{s_2} \eta ds \geq -\frac{q}{T}|_{s_1}^{s_2}, \quad (22)$$

where  $\eta = \eta(s, t)$  is the entropy per unit length at material point  $s$  at time  $t$  and  $T$  is the system temperature. Localizing this away from the discontinuity, we get

$$\dot{\eta} + \frac{1}{T} \frac{\partial q}{\partial s} \geq 0. \quad (23)$$

We introduce the Helmholtz free energy per unit length  $W = w - T\eta$ , so that we have (following Purohit and Bhattacharya):

$$f\dot{\lambda} - \dot{W} \geq 0. \quad (24)$$

Localizing to a discontinuity at  $s = x(t)$ , multiplying the entropy inequality by  $T$ , and using (21), we get

$$\dot{\lambda}([|W|] - f[|\lambda|]) \geq 0. \quad (25)$$

This is of the form

$$f_{driv} \dot{\lambda} \geq 0, \quad (26)$$

where

$$f_{driv} = [|W|] - f[|\lambda|]. \quad (27)$$

Following Abeyaratne and Knowles, we call it the driving force. As we shall see, the driving force is a key component of the description that follows.

### 3. Phase transition-like character

As mentioned earlier, the mechanical properties of a polymeric biomolecule are largely an outcome of the thermal bombardment experienced by it. Consequently, the constitutive relation for such a material is entropic in nature. In particular, the resistance to pulling the molecule is captured by a quantity termed as the persistence length of the polymer (more accurately, the bend persistence length). The persistence length is defined as the length over which correlations in the direction of the tangent along the length of the molecule are lost. This means that in a polymer with a shorter persistence length, any part of the molecule is less likely to be affected by the parts of the molecule in its proximity. Another interpretation is that any polymer immersed in a fluid will be randomly bent by thermal motion if its contour length is greater than its persistence length. The bending stiffness,  $K_b$ , which quantifies resistance to bending, is also a function of the persistence length,

$$K_b = \xi_p k_B T, \quad (28)$$

where  $k_B$  is the Boltzmann constant and  $T$  is the absolute temperature. While this equation appears to suggest that  $K_b$  is a function of temperature, it is not so.  $K_b$  is largely independent of temperature but the persistence length depends strongly on temperature. Thus, in their product, the temperature dependence is nullified to a large extent. If we view the polymer as an isotropic and inextensible fluctuating elastic rod, then the Gibbs free energy per unit length is given by Kulic (2004), Weiner (1983):

$$g(f, T) = -f + k_B T \sqrt{\frac{f}{K_b}} + C_p T \log\left(\frac{T}{T_t}\right) + \frac{2k_B T}{L} \log\left(\frac{\sqrt{fK_b}}{4\pi k_B T}\right), \quad (29)$$

where  $f$  is the force,  $T$  is the temperature,  $T_t$  is a transition temperature,  $C_p$  is a specific heat at constant force and  $L$  is the length of the rod. We use this free energy because the temperature and the number of monomers in the molecule being considered are constant and the force is constant as the phase boundary moves through the molecule. If  $L$  is long, i.e. several times the persistence length, and  $f$  is large, then the last term in the above expression is negligible in comparison to the others. Hence, we are left with:

$$g(f, T) = -f + k_B T \sqrt{\frac{f}{K_b}} + C_p T \log\left(\frac{T}{T_t}\right). \quad (30)$$

By differentiating the free energy with respect to the force, we get the stretch  $\lambda$ :

$$\lambda = -\frac{\partial g}{\partial f} = 1 - \frac{k_B T}{2\sqrt{fK_b}}. \quad (31)$$

Similarly, by differentiating the free energy with respect to the temperature, we get entropy per unit length  $\eta$ :

$$\eta = -\frac{\partial g}{\partial T} = -k_B \sqrt{\frac{f}{K_b}} + C_p \left[1 + \log\left(\frac{T}{T_t}\right)\right]. \quad (32)$$

This provides us with the worm-like chain (WLC) formula, which we assume governs the force-extension behavior of this rod:

$$f = \frac{1}{4\beta^2 K_b (1-\lambda)^2}, \quad (33)$$

where  $K_b$  is the bending modulus, and  $\beta = 1/k_B T$ .

The above description of constitutive behavior has been found to be valid with appropriate values of the persistence length for a wide range of macromolecules. For a macromolecule that undergoes unfolding, it may be assumed to hold for the state produced after unfolding. Estimates for the persistence lengths of unfolded states or phases, as we shall refer to them in this paper, are much smaller than those for the corresponding folded phases. In certain cases, the behavior of the unfolded phases may be described by other constitutive laws. However, in this paper, we have assumed that the worm-like chain relation describes the behavior of both phases.

The introduction of two phases via a structural change leads us to the question whether unfolding in macromolecules may be considered as a first order phase transition. Interestingly, even though it is not considered a true phase transition (due to the molecule being a one-dimensional object (Grosberg and Khokhlov, 2002)) DNA overstretching has been shown to follow a form of the Clausius–Clapeyron equation (Nelson, 2004). This form is

$$\frac{df}{dT} = -\frac{\eta_u - \eta_f}{\lambda_u - \lambda_f}, \quad (34)$$

where  $\eta_u$ ,  $\eta_f$ ,  $\lambda_u$  and  $\lambda_f$  are the entropy per unit length and stretch values for the unfolded and folded phases, respectively. Hereafter, we shall use the subscripts  $u$  and  $f$  to denote quantities in the unfolded and folded phases. In order to test the assumptions of our model vis-a-vis this feature of DNA overstretching, we show here that the assumptions produce results in agreement with other independent analyses. We use Eqs. (31) and (32) to find expressions for  $\eta_u$ ,  $\eta_f$ ,  $\lambda_u$  and  $\lambda_f$ . In addition to the entropy per unit length expression obtained from (32), there is a term which accounts for the change associated with a latent heat absorbed in moving from the folded to the unfolded state. Accounting for this term, we get

$$\eta_u = -k_B \sqrt{\frac{f}{K_u}} + C_{p,u} \left( 1 + \ln \frac{T}{T_t} \right) + \eta_L \quad (35)$$

for the unfolded phase. Here,  $T_t$  is the transition temperature, and  $\eta_L = L_t/T_t$  is the entropy change per unit length of the unfolded phase at  $T_t$ , involving the transfer of latent heat  $L_t$ . The overstretching transition takes place at  $T_t$ . Similarly, for the folded phase,

$$\eta_f = -rk_B \sqrt{\frac{f}{K_f}} + C_{p,f} \left( 1 + \ln \frac{T}{T_t} \right), \quad (36)$$

where  $r$  is the ratio of distances between adjacent monomers in the folded to that in the unfolded phase. It is obviously less than unity. Here, we assume that the specific heats of both phases are the same, i.e.  $C_{p,u} = C_{p,f} = C_p$ . The stretches are given by

$$\lambda_u = -\frac{\partial}{\partial f} \left( -f + k_B T \sqrt{\frac{f}{K_u}} \right) = 1 - \frac{k_B T}{2\sqrt{fK_u}} \quad (37)$$

and

$$\lambda_f = -\frac{\partial}{\partial f} \left[ r \left( -f + k_B T \sqrt{\frac{f}{K_f}} \right) \right] = r \left( 1 - \frac{k_B T}{2\sqrt{fK_f}} \right). \quad (38)$$

Substituting these values in (34), we get the equation for the phase coexistence line on the  $f-T_t$  plane:

$$\frac{df}{dT_t} = -\frac{-k_B \sqrt{\frac{f}{K_u}} + \eta_L + rk_B \sqrt{\frac{f}{K_f}}}{1 - \frac{k_B T}{2\sqrt{fK_u}} - r \left( 1 - \frac{k_B T}{2\sqrt{fK_f}} \right)}, \quad (39)$$

since the Clausius–Clapeyron equation gives the change of the transition temperature with applied force in a first order phase transition. Rearranging terms, we obtain:

$$\frac{df}{dT_t} = \frac{\eta_L - B\sqrt{f}}{\frac{BT_t}{2\sqrt{f}}(1-r)}, \quad (40)$$

where the constant  $B$  is given by

$$B = k_B \left( \frac{1}{\sqrt{K_u}} - \frac{r}{\sqrt{K_f}} \right). \quad (41)$$

For DNA, the accepted values of these quantities are  $r=0.586$ ,  $K_f = 50k_B T$  pN nm<sup>2</sup> and  $K_u = 0.75k_B T$  pN nm<sup>2</sup> at  $T=300$  K. This equation can be numerically integrated with  $\eta_L$  as the lone fit parameter. We have found that  $\eta_L = 16.7$  cal/mol K yields a very good fit to the experimental data of Williams et al. (2002) (Fig. 3). This result confirms our belief that the quasistatic picture of a partially unfolded molecule that we have considered is a suitable choice for the study of the evolution of this system. Our claim is not that the overstretching transition is a true phase transition, but rather that results developed for phase transitions in one-dimensional continua have potential to be applied to its study. Also, the excellent agreement with prior published results obtained from completely different analysis cannot be coincidental. Hence, we proceed towards setting up the equations that will allow us to analyze how this system develops over time, under different conditions.

#### 4. Molecular stretching with no phase change

The next step in the development of the model is to use Eqs. (33) and (8) to solve for the temporal behavior of the two unknowns  $f$  and  $z$ . The drag coefficient  $d_w$  is estimated by Brennen and Winet (1977) formula introduced earlier in Eq. (6). Our first step was to establish the appropriateness of this formula for modeling experiments. We considered the

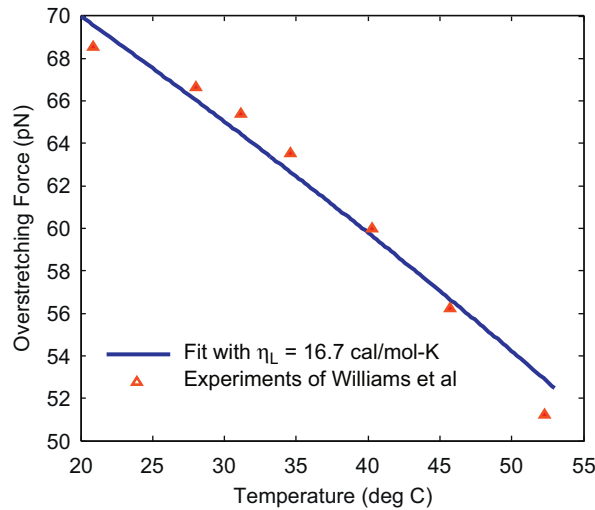


Fig. 3. Comparison of predictions from the model based on Clausius–Clapeyron equation with experimental results of Williams et al. (2002).

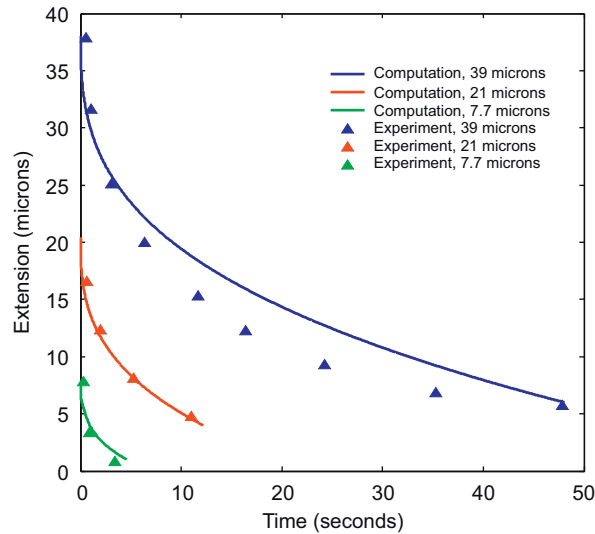


Fig. 4. Comparison with experimental data of Perkins et al. (1994). A single drag coefficient has been used, and one end is fixed while the other is a free end. Fluid velocity is zero.

experimental data of Perkins et al. (1994). They analyzed single molecules of DNA by stretching them to full extension and then measured their relaxation in a quiescent fluid. This data provided a simple case for our program to model. The authors provided results for three different DNA lengths and also specified the viscosity of the solution in which the molecules were placed. Therefore, by using the values  $\mu = 15$  cp,  $a = 1$  nm, and lengths,  $2l = 39.1$ ,  $21.1$  and  $7.7$   $\mu\text{m}$ , we aimed to reproduce the experimental results.

The boundary conditions for this experiment are  $f(L_c, t) = 0$  and  $z(0, t) = 0$  implying zero force at one end and a zero displacement at the other. Since the equation is a nonlinear PDE, we solve it numerically using a finite difference method. The initial condition was a uniform stretch in the entire molecule. This stretch was computed by dividing the maximum length on each curve by the contour length. The estimate for the drag coefficient is then plugged in and the system is solved.

The comparison is shown in Fig. 4. We not only get a very close correspondence with experimental results, but also observe that the curves agree remarkably well for a single value of the drag coefficient as found from the Brennen–Winet formula. This tells us that this simple computation provides us with a value that is quite conveniently usable for all experiments with the same molecule–fluid system. We also see that while the agreement is almost exact for higher extensions, it is less so when the molecule has relaxed to about half of its length. This is admittedly not the range at which the abstracted worm-like chain relation or the Brennen–Winet formula are at their best at predicting the extension or the drag coefficient.

Even though the general system does not admit a solution in the form of a convenient expression, it can be solved analytically for a few special cases. We want to use the solution to such a case to note how accurate our computation is, and also to reassure ourselves that the error decreases as we decrease the element size in the computation. One of these special cases is a molecule that is allowed to come to steady state under the influence of a flowing fluid. Such a scenario is easily obtained in the case of a molecule being stretched out in a microfluidic channel. Under these circumstances, there is no dependence of any quantity on time, and the system can be solved easily. We start with the force balance equation (8), and put  $\partial z/\partial t$  equal to zero. This gives us,

$$\frac{df}{ds} = -d_w v, \quad (42)$$

which when integrated becomes

$$f = -d_w v s + C_1 \quad \text{or} \quad f = C_1 - C_2 s, \quad (43)$$

where  $C_2 = d_w v$ . To determine the constant of integration  $C_1$ , we recognize that at the fixed end of the molecule, the support will exert a reaction on the molecule equal to the cumulative drag force exerted by the fluid along the molecule. From this, we get

$$C_1 = f(0) = d_w v L_c, \quad (44)$$

where  $L_c$  is the contour length of the molecule (this notation will be used to distinguish it from the observed length of the molecule,  $L$ , hereafter). The constitutive equation (33) can now be written as

$$dz = \left(1 - \frac{1}{2\beta\sqrt{f}K_b}\right) ds \quad \text{or} \quad dz = \left(1 - \frac{C_3}{\sqrt{f}}\right) ds, \quad (45)$$

where  $C_3 = 1/2\beta\sqrt{K_b}$ . Now, we substitute (43) into the above expression and integrate to get:

$$z = s + \frac{2C_3}{C_2} \sqrt{C_1 - C_2 s} + C_4, \quad (46)$$

where  $C_4$  is a constant of integration. Its value is found by requiring that the displacement at  $s=0$  be zero, or  $z(0) = 0$ . This gives us

$$C_4 = -\frac{2C_3}{C_2} \sqrt{C_1}. \quad (47)$$

Hence, we can write, after substituting the constants  $C_1$ ,  $C_2$  and  $C_3$ ,

$$z = s + \frac{1}{\beta\sqrt{K_b d_w v}} \left(\sqrt{L_c - s} - \sqrt{L_c}\right). \quad (48)$$

This expression provides us a baseline to compare the results of our computation with. Knowing the exact description of the steady state, we now compute the error that our computation has in comparison with this steady state. We compute two kinds of errors, the  $L^2$  error and the maximum error. These are given by

$$L^2 \text{ error} = \sqrt{\sum_{i=1}^N (u_e(i) - u_c(i))^2} \quad (49)$$

and

$$\text{Maximum error} = \max(|u_e - u_c|), \quad (50)$$

where  $u_e$  is the exact position of the node  $i$  at steady state, obtained from (48),  $N$  is the number of nodes, and  $u_c$  is the computed position from our finite difference method. Shown in Fig. 5 is the progression of the error as a function of the number of discretized elements in the molecule. As expected, both the  $L^2$  error, and the maximum error decline as the element size becomes smaller.

The steady state solution worked out above is particularly useful in establishing the accuracy of our numerical scheme. However, it is equally interesting to note the evolution of the system from an initial, specified condition. We have shown in Fig. 6 the temporal variation of the strain in different parts of the molecule as it evolves to steady state. There are several features of interest here. The strain can always be seen to be maximum at the fixed end, which is expected, since the drag force is distributed along the length of the molecule. Also, we see that the molecule starts experiencing strain from the fixed end and a wave of increasing strain moves through the molecule before reaching the steady state profile. Fig. 6 also shows the evolution of force in the molecule. Corresponding to the evolution of stretch, the force is also greatest at the fixed end. Also noteworthy is the fact that the force profile is linear in steady state, as expected.

Experiments have also been performed in which the fluid velocity is either not constant, and/or the molecule is not fixed at one end. In our computation scheme, we are able to prescribe spatial variations of velocity, as shown in Fig. 7. For a molecule moving with fluid flow, it is assumed that the trailing end of the molecule moves with the fluid velocity, while the leading end feels zero tension. This would be the case if, for instance, the trailing end is attached to a spherical bead

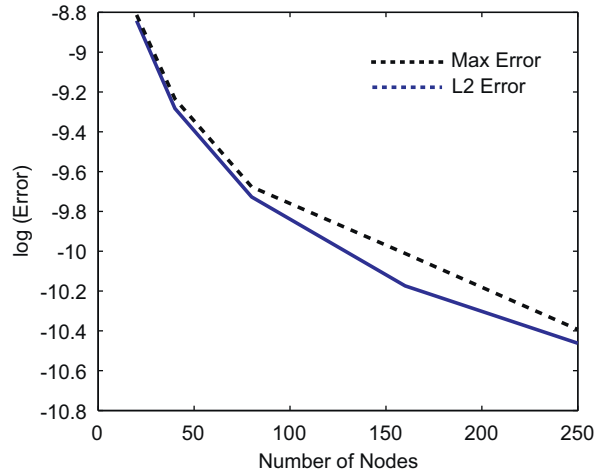


**Fig. 5.** Variation of the log of the error with the number of nodes in the numerical scheme used. The error is computed using the analytical steady state solution for a molecule stretched in a fluid flowing at velocity  $v$ .

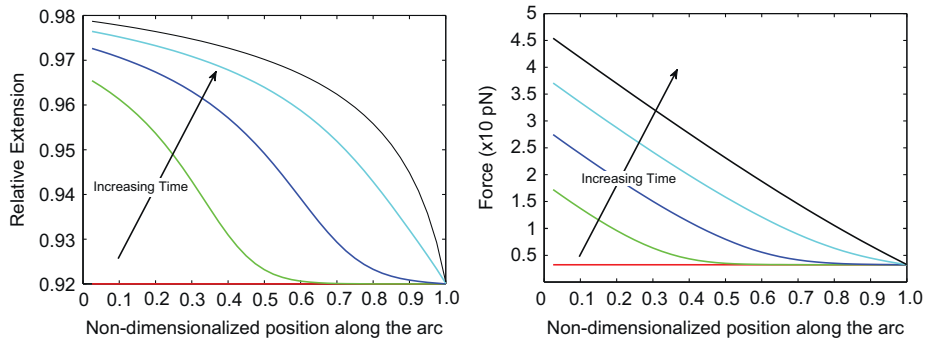


**Fig. 6.** (left) Depiction of how the molecule elongates under the influence of a constant extensional flow. Note that because of the fixed end boundary condition at  $s=0$ , the maximum strain is at that end. (right) Variation of the force along the molecule that elongates in an extensional flow. The force is maximum at the fixed end, where the maximum strain is also present. In addition, the force profile is linear after steady state has been achieved, which is as per our expectation.

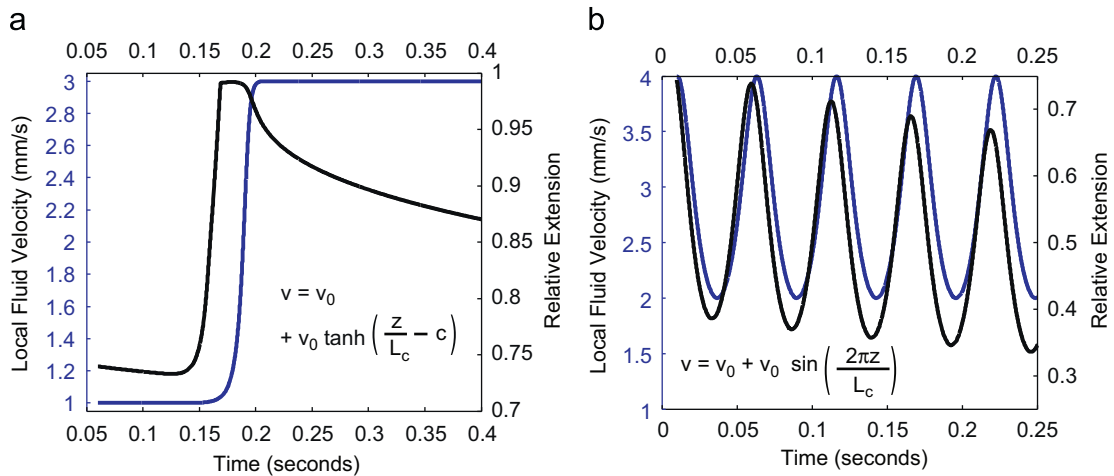


**Fig. 7.** (a) Variation of velocity and extension upon imposing a step velocity profile. The step has been simulated by a hyperbolic tangent function for the velocity. Note that the extension occurs only while the velocity is increasing. In the two regions where the fluid is moving at a constant speed, the molecule has no force gradient acting on it. Hence, it tends to move towards a low-strain state. (b) Variation of velocity and extension upon imposing a sinusoidal fluid velocity field on the molecule. Note the difference of phase between the two curves, which is in keeping with the dissipative nature of the process.

which moves with the fluid velocity. In Fig. 7(b), the extension of the molecule is plotted against an imposed sinusoidal fluid velocity. As expected, the extension follows the velocity, but with a phase lag. This is the sign of a dissipative process, which is indeed embodied in the governing equations. A similar plot with the molecule moving in a fluid stream in a microchannel that produces a step-like variation in the fluid velocity (Fig. 7(a)). The  $\tan^{-1}$  function is used to model this step. This plot differs from the previous figures in that the extension begins to decay when the velocity becomes constant away from the step. It is reiterated from these plots that uniform flow cannot cause extension on its own in a molecule that is free to move with the flow. A force gradient is essential for stretching. In the absence of a force gradient along its length, the molecule decays to a shorter length, the rate of decay increasing with a decrease in  $d_w$ .

## 5. Molecular stretching with unfolding via interface propagation

Extending the single-phase model to a two-phase model requires introducing the constitutive law for the second phase and a framework to handle the variation of quantities across the interface or discontinuity between the phases. For this, we shall use the Abeyaratne–Knowles theory of phase transitions (Abeyaratne and Knowles, 2006). In the experiments under consideration, each part of the molecule experiences the same force, while the strain is different depending on the local phase. The Abeyaratne–Knowles theory deals with similar transitions in one-dimensional continua. Such systems have been shown by Ericksen (1975) to be describable by a nonmonotonic stress–strain relation. This continuum is termed as a phase mixture, and the interfaces between phases, assumed to be well-defined, are called phase boundaries. Given the close correspondence between this theoretical picture and experimental observations in macromolecules, this theory was chosen to model behavior at the discontinuity.

As stated earlier, we assume that the two phases follow the worm-like chain constitutive relation, but with different persistence lengths. The expressions for tension in the low-strain and high-strain phases become

$$f = \begin{cases} \frac{1}{4\beta^2 K_f \left(1 - \frac{\lambda}{r}\right)^2} & \text{for low-strain phase} \\ \frac{1}{4\beta^2 K_u (1 - \lambda)^2} & \text{for high-strain phase,} \end{cases} \quad (51)$$

where  $K_f$  and  $K_u$  are the bending moduli for the low- and high-strain phases, respectively.  $\lambda$  is the stretch with respect to the reference (fully stretched state in the completely unfolded phase) configuration. The parameter  $r$  is the ratio of fully stretched folded and unfolded lengths of the same segment of the molecule. It is noteworthy that the parameter  $r$  is a surrogate for the transformation strain  $\gamma_T$  used in the Abeyaratne–Knowles theory.

The behavior at the interface of physical quantities of interest to us is given by jump conditions, which follow from the Abeyaratne–Knowles theory. These are the kinematic and force jump conditions, Eqs. (1) and (9). We note that besides displacement and tension, all other physical quantities of interest, such as the energy density, the local velocity and the strain are also discontinuous, and in general, not the same on either side of the discontinuity. These relations specify the properties of the physical quantities on either side of the interface.

When we consider the evolution of the interface, two questions arise: first, what conditions are required to be satisfied for the interface to appear, or nucleate, and second, what determines how this interface propagates. The Abeyaratne–Knowles theory specifies two fundamental conditions for the existence and propagation of this interface. The first of these is a *nucleation criterion*. We assume simply that the phase boundary appears when a certain force is reached at a point along the molecule. This is our nucleation criterion. In addition, for simplicity, we also assume that there can only be one interface present in a macromolecule at a time. Justification for this assumption lies in what is called high cooperativity. This shall be discussed later in the paper. As shown earlier, the force is maximum at the end which is being pulled, and decreasing monotonically along the molecule (for an experiment in which one end is kept fixed and the other end is pulled away at constant velocity). Therefore, the nucleation force is first achieved at the end being pulled, and this is where we will nucleate the interface in the majority of scenarios considered hereafter. This has been observed in the experiments of van Mameren et al. (2009) as well. We note here that this need not always hold. Parts of a macromolecule are distinguishable when looked at closely. Even in the case when we are looking at it macroscopically, there are defects in molecules that make these particular sites much more conducive to the origination of the discontinuity. At the same time, the design of the experiment may also dictate the location of the nucleation site.

The second required condition is the *kinetic relation*. The kinetic relation specifies the way in which the velocity of the phase boundary varies with the thermodynamic driving force (which is, in general, different from the mechanical force felt at the interface) across it, i.e.  $\dot{x} = \dot{x}(f_{driv})$ . According to the Abeyaratne–Knowles theory, the driving force is given by

$$f_{driv} = [|W|] - f_x[|\lambda|], \quad (52)$$

where  $W$  is the stored energy per unit length,  $f_x$  is the tension in the molecule at the phase boundary (same on either side) and  $\lambda$  is the stretch.  $W$  is calculated using

$$W = \int_{\lambda_{min}}^{\lambda} f(\lambda') d\lambda', \quad (53)$$

where  $f(\lambda)$  is obtained from (51). For the high-strain phase, in addition to the integral above we include the average energy per unit length  $W_B$  required to facilitate the transition from the low-strain phase. The choice of the parameter  $W_B$  requires further elucidation. A large body of current opinion in the biophysics community says that the resultant state of the DNA overstretching transition is the single-stranded state. There is conflicting evidence on this point. The Gibbs free energies for both the single stranded state and the native double-helical B-DNA are available. From available data (Rouzina and Bloomfield, 2001), we see that at the transition force of 65 pN and  $T=300$  K, the expected Gibbs energy difference is between the limiting values of  $1.1k_B T$  per base pair and  $2.3k_B T$  per base pair. We choose to take the value of  $W_B$  to be the average of these values, i.e.  $1.7k_B T$ .  $W_B$  is related to the latent heat  $L_t$  mentioned earlier.

Prior to making this choice, we considered the transition to be a melting-like transition as discussed above. However, the value of  $W_B$  computed by assuming that bonds were being completely broken was about 30 times the average value chosen above (Yanson et al., 1979). The reason for this discrepancy is that each base pair is bound via AT or GC hydrogen bonds, which account for about  $6-10k_B T$  of binding energy, and there is about  $10-20k_B T$  per bp of binding enthalpy due to a phenomenon called base stacking. Base stacking further reduces the energy of the helix by bond formation between the loops of the helix stacked on top of one another. It is largely an electrostatic interaction. Despite their differences regarding the mechanism of the transition, most modeling studies agree that it is possible to extend double-stranded DNA to about twice its B-form contour length, while maintaining most of the hydrogen bonding and giving up only about half of the base stacking interactions. Thus, while energy is lost due to the breaking of the bonds, much of the base stacking interactions remain. Their difference is about  $2k_B T$ , which is about an order of magnitude smaller than either. Therefore, the assumption of complete bond-breaking being at the heart of the DNA overstretching transition appears to be inaccurate, and we do not set  $W_B=L_t$ .

For other parameters in the formula, we choose  $\lambda_{min}$  to be the lower limit of the stretch at which the WLC formula for the force-extension behavior of the polymer can be applied and  $\lambda$  is the current stretch which is equal to  $\lambda_f$  in the low-strain phase and  $\lambda_u$  in the high-strain phase. It is noteworthy that the strains  $\lambda_f$  and  $\lambda_u$  are functions of the tension at the interface (as given by (51)), and hence, the driving force is a function of only the tension at the interface. This can be shown as follows.

We start with the formula for the thermodynamic driving force given by (52). Identifying the + phase as unfolded and – phase as folded, we now find expressions for the stored energies per unit length. For the unfolded phase,

$$f = \frac{1}{4\beta^2 K_u (1-\lambda)^2}, \quad (54)$$

which gives us, for the stored energy per unit length,

$$W_u = \int_{\lambda_m}^{\lambda_u} \frac{1}{4\beta^2 K_u (1-\lambda')^2} d\lambda' + W_B. \quad (55)$$

For the folded phase, we similarly have

$$W_f = \int_{\lambda_m}^{\lambda_f} \frac{1}{4\beta^2 K_f \left(1 - \frac{\lambda''}{r}\right)^2} d\lambda''. \quad (56)$$

Performing these integrals yields,

$$W_u = \frac{1}{4\beta^2 K_u} \left[ \frac{1}{1-\lambda_u} - \frac{1}{1-\lambda_m} \right] + W_B, \quad (57)$$

$$W_f = \frac{r}{4\beta^2 K_f} \left[ \frac{1}{1 - \frac{\lambda_f}{r}} - \frac{1}{1 - \frac{\lambda_m}{r}} \right]. \quad (58)$$

Using the fact that the force  $f$  can be written as a function of either of the strains, and substituting  $4\beta^2 K_u = 1/C_u$  and  $4\beta^2 K_f = 1/C_f$ , we have

$$f_d = C_u \left[ \frac{1}{1-\lambda_u} - \frac{1}{1-\lambda_m} \right] + W_B - r C_f \left[ \frac{1}{1 - \frac{\lambda_f}{r}} - \frac{1}{1 - \frac{\lambda_m}{r}} \right] - \frac{C_u}{(1-\lambda_u)^2} (\lambda_u - \lambda_f), \quad (59)$$

or, grouping constant terms together,

$$f_d = C_m + \frac{C_u}{(1-\lambda_u)^2} (1-2\lambda_u + \lambda_f) - \frac{rC_f}{1-\frac{\lambda_f}{r}}. \quad (60)$$

Since the strains are functions of force only:

$$\lambda_f = r \left( 1 - \sqrt{\frac{C_f}{f_x}} \right) \quad \text{and} \quad \lambda_u = 1 - \sqrt{\frac{C_u}{f_x}}, \quad (61)$$

we conclude that the thermodynamic driving force is a function of only the force at the interface.

From the outset, one of the aims of this work has been to introduce time scales into the description of the unfolding process, so that we are able to study and account for rate effects observed in experiments. The kinetic relation, understood most simply, is what causes the interface to move at a particular speed, given the local stress and strain conditions. Consequently, the kinetic relation proves to be the pivotal parameter in this study. In what follows, we shall consider a number of relations and demonstrate how they change the response of the system to conditions which are unchanged. We will begin with a simple kinetic model and move to more involved models.

The first application for our framework is in the reproduction of the plateau-like force response shown earlier. Similar to the one-dimensional case, we integrate (8) together with the force-stretch relation (51), but allow for one phase boundary whose position in the reference configuration is  $x(t)$ . The boundary conditions remain the same:

$$\dot{z}(L_c, t) = v_p, \quad z(0, t) = 0, \quad (62)$$

where  $v_p$  is a pulling velocity imposed at one end of the molecule. At  $t=0$ , the entire molecule is assumed to be in the low-strain phase. The fluid velocity is zero. As a result, as long as the force in the molecule has not equilibrated, it will be a maximum at  $s = L_c$ . As discussed earlier, the phase boundary is nucleated at  $s = L_c$  when the tension there reaches a threshold.

The subsequent motion is governed by the kinetic relation. However, in the case at hand, since we impose the condition that the applied force (and hence, the force at the interface) remains constant (the main feature of a plateau-type force response), we also require that the driving force should stay constant. Clearly, the choice of a particular kinetic relation is redundant here, since the speed of the interface would also be constant. Therefore, in place of a kinetic relation, we impose a constant interface speed. The choice of this constant speed is discussed later in the paper.

The discretization scheme used in the single phase system would not be useful in this case because we want to calculate local values of quantities and impose jump conditions at the interface. For this, we modify our finite difference numerical scheme to account for the presence of the moving phase boundary by adding a mobile node to our existing discretization scheme and computational method (Purohit and Bhattacharya, 2003). This node is attached to the moving interface. Due to this, at a particular time, only one element in the discretized continuum has two parts, one in each phase. Using the constitutive laws for the two phases, the force jump condition (9) reduces to

$$\left( 1 - \frac{\lambda_f}{r} \right) = \sqrt{\frac{K_u}{K_f}} (1 - \lambda_u), \quad (63)$$

where  $\lambda_f$  and  $\lambda_u$  are the stretches in the low- and high-strain phases, respectively, right next to the interface. In our finite difference scheme the stretches  $\lambda_f$  and  $\lambda_u$  can be expressed in terms of the position of the discontinuity  $z_x$  (in the deformed

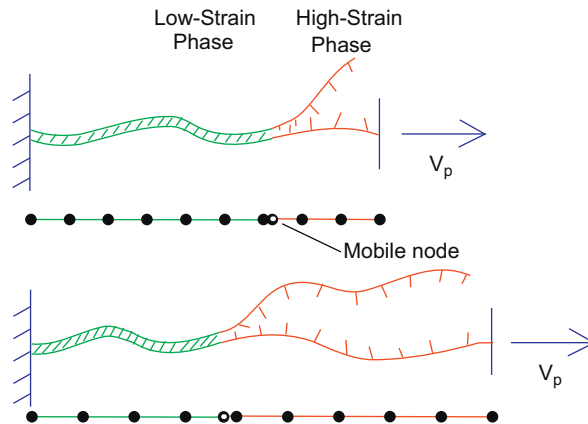


**Fig. 8.** A schematic representation of the model. The molecule is represented by a one-dimensional continuum (lines underneath the cartoon of the partially unfolded molecule) with an interface separating two metastable phases. Black circles in the one-dimensional continuum indicate nodes used in the numerical scheme. Open circles indicate position of the interface. One end of the molecule is fixed while the other is pulled at a constant velocity. (For interpretation of the references to color in this figure legend, the reader is referred to the web version of this article.)

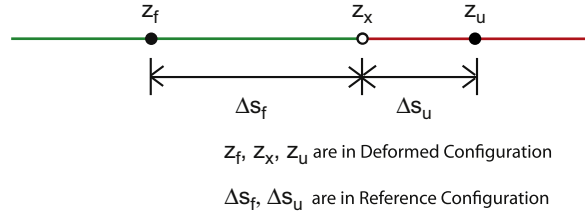


**Fig. 9.** Nodes represented by  $z_f$  and  $z_u$  are fixed in the reference configuration, while the extra node for the interface, represented by  $z_x$ , is a moving node. Also shown are the variable length sub-elements,  $\Delta s_f$  and  $\Delta s_u$ , which are such that  $0 \leq \Delta s_f, \Delta s_u \leq \Delta s$ .

configuration) and the positions of higher and lower nodes,  $z_u$  and  $z_f$ , respectively, as (see Fig. 9)

$$\frac{\lambda_f}{r} = \frac{z_x - z_f}{r \Delta s_f} \quad \text{and} \quad \lambda_u = \frac{z_u - z_x}{\Delta s_u}, \tag{64}$$

where  $\Delta s_f + \Delta s_u = \Delta s$  is the distance separating two nodes bracketing the node representing the moving phase boundary in the reference configuration. We prefer to formulate these expressions in terms of quantities that are known. The position of the interface is not generally known, and can only be calculated from other quantities. Thus, eliminating  $z_x$  between (63) and (64), we obtain

$$\lambda_f = \frac{\sqrt{K_u}(z_u - z_f) + \Delta s_u(\sqrt{K_f} - \sqrt{K_u})}{(\sqrt{K_u}r\Delta s_f + \sqrt{K_f}\Delta s_u)}, \tag{65}$$

$$\lambda_u = \frac{\sqrt{K_f}(z_u - z_f) + r\Delta s_f(\sqrt{K_u} - \sqrt{K_f})}{(\sqrt{K_u}r\Delta s_f + \sqrt{K_f}\Delta s_u)}. \tag{66}$$

Note that we assume  $z(s^+(t), t) = z(s^-(t), t) = z_x$  is continuous, hence the kinematic jump condition is automatically satisfied.

We also note that any transition taking place must be shown to satisfy the second law of thermodynamics. The second law for phase transitions is formulated in terms of the thermodynamic driving force,

$$D = f_{driv} \dot{x} \geq 0. \tag{67}$$

The quantity  $D$  is the rate of dissipation associated with the motion of a phase boundary through a continuum (Abeyaratne and Knowles, 1990). It is defined as the product of the thermodynamic driving force with the interface velocity, both appropriately signed ( $\dot{x}$  is positive if it moves from smaller to larger values of arc length  $s$ ). If the rate of dissipation is negative, the motion is aphysical and cannot occur. We ensure that this is always satisfied in our computations.

### 6. Results

We now come to the choice of the constant interface speed mentioned earlier. In experimental studies, the pulling velocity is often a controllable parameter. For a phase change process in which the force remains constant, the interface speed is likely to be a function of both force and pulling velocity. To find a relation between the pulling velocity and the interface speed, we began with the assumption that the process was quasistatic, and start with the equations for lengths of the chain in the folded and unfolded phases. These are

$$L_f = rL_c \left( 1 - \frac{1}{2\beta\sqrt{fK_f}} \right) n_f, \tag{68}$$

$$L_u = L_c \left( 1 - \frac{1}{2\beta\sqrt{fK_u}} \right) n_u. \tag{69}$$

We recall here, that  $r$  is the ratio of a fully extended segment of the chain in the *folded* configuration to its length when fully unfolded and stretched out.  $L_c$  is the contour length in the fully unfolded state, and  $n_f$  and  $n_u$  are the arc length fractions of the chain in folded and unfolded states, respectively.  $f$  is the applied force. It is worth noting that  $f$  is assumed to be constant all along the chain, since this is a quasistatic process. The length of the chain is the sum of these lengths,

$$z(L_c, t) - z(0, t) = L_f + L_u = L_c \left[ (m_f + n_u) - \frac{1}{2\beta\sqrt{f}} \left( \frac{n_u}{\sqrt{K_u}} + \frac{m_f}{\sqrt{K_f}} \right) \right]. \tag{70}$$

We now differentiate the above equation with respect to time to get,

$$\frac{\dot{z}(L_c, t) - \dot{z}(0, t)}{L_c} = r \frac{dn_f}{dt} + \frac{dn_u}{dt} + \frac{1}{4\beta f^{3/2}} \left( \frac{n_u}{\sqrt{K_u}} + \frac{rn_f}{\sqrt{K_f}} \right) \frac{df}{dt} - \frac{1}{2\beta\sqrt{f}} \left( \frac{dn_u}{dt} \frac{1}{\sqrt{K_u}} + \frac{dn_f}{dt} \frac{r}{\sqrt{K_f}} \right). \quad (71)$$

In the case of a plateau, the force  $f$  remains constant with time as the interface moves along the molecule. Thus,  $df/dt = 0$ , and we get

$$\frac{\dot{z}(L_c, t) - \dot{z}(0, t)}{L_c} = r \frac{dn_f}{dt} + \frac{dn_u}{dt} - \frac{1}{2\beta\sqrt{f}} \left( \frac{dn_u}{dt} \frac{1}{\sqrt{K_u}} + \frac{dn_f}{dt} \frac{r}{\sqrt{K_f}} \right). \quad (72)$$

We fix the end  $s=0$ , therefore  $\dot{z}(0, t)=0$ . Also, since  $n_f + n_u = 1$ , we have  $dn_f/dt = -dn_u/dt$ , which simplifies the above equation to

$$\frac{\dot{z}(L_c, t)}{L_c} = \frac{dn_f}{dt} \left[ (r-1) - \frac{1}{2\beta\sqrt{f}} \left( \frac{r}{\sqrt{K_f}} - \frac{1}{\sqrt{K_u}} \right) \right]. \quad (73)$$

We recognize that the product of contour length  $L_c$  and folded fraction  $n_f$  is the arc length in folded state. Therefore, the term  $L_c(dn_f/dt)$  is equal to the interface speed when there is only one interface, which when positive (in our chosen coordinate system) moves from  $s=0$  to  $L_c$ . Thus, we have,

$$L_c \frac{dn_f}{dt} = \dot{x}. \quad (74)$$

Also, we note that the term  $\dot{z}(L_c, t) = v_p$ . This gives us the expression we require:

$$\frac{v_p}{\dot{x}} = (r-1) - \frac{1}{2\beta\sqrt{f}} \left( \frac{r}{\sqrt{K_f}} - \frac{1}{\sqrt{K_u}} \right), \quad (75)$$

or, its reciprocal,

$$\frac{\dot{x}}{v_p} = \frac{1}{(r-1) - \frac{1}{2\beta\sqrt{f}} \left( \frac{r}{\sqrt{K_f}} - \frac{1}{\sqrt{K_u}} \right)}. \quad (76)$$

This expression tells us that the interface speed is a constant for a given plateau force and pulling velocity combination. We tested this result by plugging in the interface speed values predicted into our computation. Four different pulling velocities (0.3, 0.7, 1.5 and 3.0  $\mu\text{m/s}$ ) and four different plateau forces were tested. As the interface propagates,  $\dot{x}$  is set as a fixed speed. We find that the predicted speed indeed leads to plateaus, thus validating both the near-equilibrium hypothesis, as well as the mobile node numerical scheme implemented (Raj and Purohit, 2010). We find the force-stretch response for different values of the plateau tension, for unfolding as well as refolding transitions, with pulling velocity  $v_p = 3 \mu\text{m/s}$ . In each of these cases, we employ a different, but constant  $\dot{x}$ , in accordance with the predicted value in (76). We note that this phase-transition based model handles extremely well all the parts of the force-stretch curve (see Fig. 10), including the early pliability, the stiffening at high extensions, and the structural transition. We also compared results from our computation with available unfolding results for DNA and these comparisons are very good, as seen in Fig. 10. It is also noteworthy that the model accurately reproduces experimental data for other molecules such as myosin (Raj and Purohit, 2010). We have also shown in Fig. 10, a simple representation of hysteresis which has been observed in several experiments in which unfolding and subsequent refolding were allowed to occur. The initiation of these processes at different forces is sufficient for hysteresis to take place.

We note that these results imply that the dissipation, as defined in (67), is a constant for a given plateau force  $f_x$ , or

$$D = f_{driv} \dot{x} = D_S = D_S(f_x). \quad (77)$$

With the chosen values of  $W_B$  and material parameters  $K_u$ ,  $K_f$  and  $r$ , we find that the dissipation is negligible as compared to the rate of work done on the molecule at the boundary  $s = L_c$  for the 65 pN plateau. This is consistent with the idea that most of the work is stored as elastic energy in the molecule and that the process is quasistatic. We point out that though the force plotted in the force-extension curve is the force experienced at the end of the molecule, not the force at the interface, these two forces are so close to each other for fluid viscosities used in our computations, that, they can be used interchangeably.

Having asserted that only specific combinations of  $\dot{x}$  and  $v_p$  yield plateaus, the next question is, how does the behavior change for combinations other than these? We expect that in these scenarios, we should not see plateaus being formed, and that is indeed the case. As previously shown by Raj and Purohit (2010), the plateau-like behavior persists, but with an important difference. When the nucleation force remains fixed, and the  $\dot{x}/v_p$  is varied, the force-extension curves eventually approach a plateau at the force at which the unfolding would have had to be nucleated to get a plateau for that value of  $\dot{x}/v_p$ . So, if  $\dot{x}/v_p$  for a transition nucleating at 65 pN is higher than the value that produces a plateau at 65 pN, then the force-extension curve tends to a plateau lower than 65 pN. This plateau occurs at approximately the same force at which our chosen  $\dot{x}/v_p$  is predicted to form a plateau, if nucleated at that force. We also did computations for the

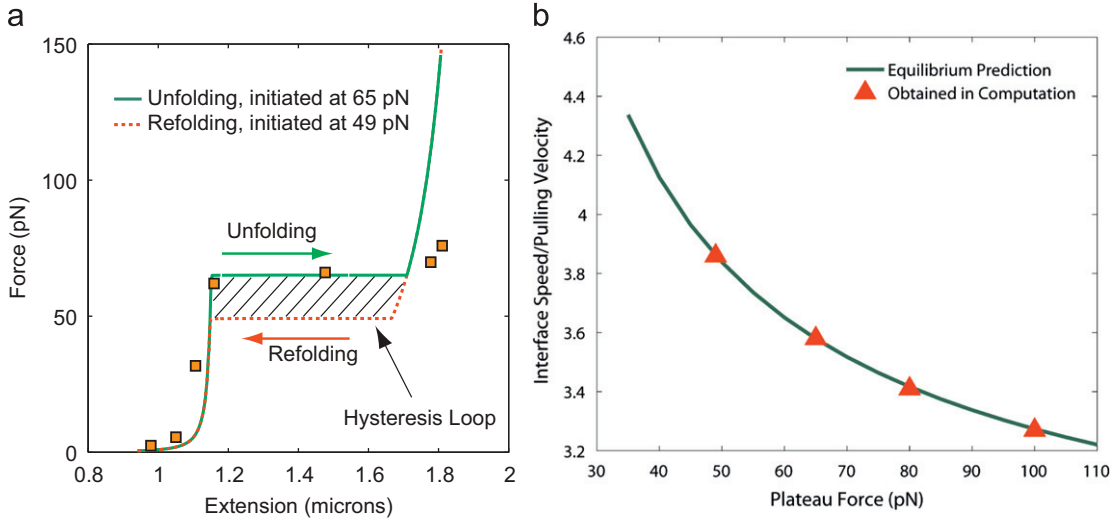


**Fig. 10.** (a) Force-extension curves produced by the model. Both unfolding and subsequent refolding are demonstrated. The forward transition was nucleated at 65 pN, and the reverse was nucleated at 49 pN. The interface propagation model is able to reproduce all parts of the force-extension curve. Hysteresis between the two curves is also shown. The black-orange squares are experimental results of Smith et al. (1996), scaled to the axes shown. The parameters are  $K_f=50$  nm,  $k_B T$  and  $K_u=0.75$  nm,  $k_B T$  at  $T=300$  K. (b)  $\dot{x}/v_p$  calculated from Eq. (76) (green curve) compared to values that generate plateaus in the computation (red triangles). (For interpretation of the references to color in this figure legend, the reader is referred to the web version of this article.)

complementary case: in which the  $\dot{x}/v_p$  is kept constant, while the nucleation force is varied. In this case, we found that regardless of the nucleation force, the force-extension curves tend to be the same force as long as the  $\dot{x}/v_p$  is the same.

We attempted to account for this behavior by deriving a relationship between force at the interface and the length of the molecule, while it is undergoing quasistatic unfolding. We start again with the fact that the length of the molecule is the sum of its folded and unfolded parts, in the form shown in Eq. (70), and substitute  $n_f = 1 - n_u$  to get

$$\frac{L}{L_c} = n_u \left[ (1-r) + y \left( \frac{r}{\sqrt{K_f}} - \frac{1}{\sqrt{K_u}} \right) \right] + r \left( 1 - \frac{y}{\sqrt{K_u}} \right), \quad (78)$$

where  $y = 1/2\beta\sqrt{f}$ . We are dealing with a case in which  $\dot{x}$  is a constant, therefore we can integrate  $L_c dn_u/dt = \dot{x}$  to get  $n_u = (\dot{x}/v_p L_c)(L - L_0)$ , where  $L_0$  is the extension at which nucleation takes place. Substituting this into the above equation gives us an equation of the form

$$L = M_1 \left( \frac{M_2 + y}{M_3 + y} \right), \quad (79)$$

which when inverted gives

$$f = \left( \frac{1 - N_1 L}{2\beta N_2 L - N_3} \right)^2, \quad (80)$$

with other constants  $N_1$ ,  $N_2$  and  $N_3$  which can be worked out with simple algebra. They are composed from the physical properties ( $K_f, K_u$ ), the contour length  $L_c$ , the interface speed-to-pulling velocity ratio  $\dot{x}/v_p$  and the nucleation extension  $L_0$ . In this problem, we want to show that imposing the same  $\dot{x}/v_p$  at different nucleation forces (and hence different  $L_0$ ) leads to convergent force-extension curves. We plot the analytical force-extension curve obtained using (80) and that obtained from the computation. The results are shown in Fig. 11 which demonstrate clearly that our computational method is accurate.

## 7. Other kinetic relations

Up to this point, we explored one of the simplest conditions that can be imposed on the motion of the discontinuity. A constant interface speed can recreate the force plateau in the overstretching transition of DNA and similar transitions in other macromolecules. However, it is pertinent to note that there is no reason to assume that it is the only condition that can give rise to this effect. An intrinsic feature of the force-extension curve is the absence of a time scale. It is entirely conceivable that a similar force-extension curve may result from considering other kinetic relations.

We now investigate how the imposition of other available and derived kinetic relations affect the system at hand. As before, the time scale is not entirely arbitrary, because we consider pulling speeds of the same order of magnitude as reported in experiments. This ensures that we consider physically realistic scenarios, while still allowing us to be flexible

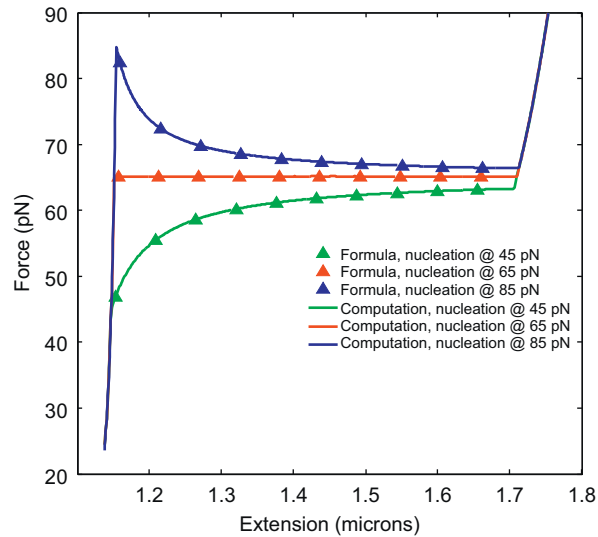


**Fig. 11.** Variation of force response for different nucleation forces, but the same interface speed, as found from our computation and from the algebraic expression (80) derived for the same.

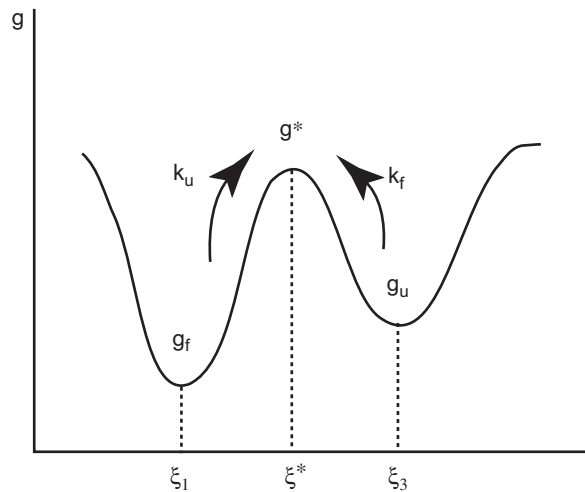


**Fig. 12.** Schematic representation of the free energy as a function of a reaction coordinate  $\xi$  for the folding-unfolding transition.

with different possible mechanisms for the interface motion. The versatility of the model and the computation technique employed allows us to handle a wide variety of kinetic relations. In addition, it can also accommodate different nucleation sites, other than the end-points of the molecule.

We are motivated to investigate a variety of kinetic relations by the intent to capture phenomena like rate-dependence and other features observed in experimental force-extension curves of rod-like molecules. We also explore connections of our work with that of predominantly thermodynamic analyses. We depart significantly from the assumptions of the previous section by treating the phase transition as single-interface motion, with the interface moving according to linear or Arrhenius kinetics. These approaches help us to make contact with previously suggested theories for propagation of phase boundaries such as those of Abeyaratne and Knowles and of Abeyaratne et al. (1996), which were not applied to rod-like molecules at all.

### 7.1. Nucleation-dominated kinetics

Let us begin with a description of a nucleation-dominated phase transition. *Nucleation-dominated* events are typically seen in materials that have a multitude of sites at which phase transformations can nucleate. When a large number of nucleation sites are available for the folding and unfolding processes, we have, for a one-dimensional continuum

(Su and Purohit, 2009) (Fig. 12):

$$\frac{dn_f}{dt} = -k_u n_f + k_f n_u, \quad (81)$$

where  $k_f$  and  $k_u$  are the rate constants for folding and unfolding, respectively.  $n_f$  and  $n_u$  are the fractions of sites available for nucleating unfolding and folding transitions, respectively. Thus (81) can be understood as giving the net rate of growth of folded units, which is equal to the instantaneous rate of folding less the instantaneous rate of unfolding. The rate of unfolding is proportional to  $n_f$  because the larger the number of folded base-pairs, the more the available sites for nucleation of the unfolded phase, and so also for the reverse transition. This assumes that there is no energetic cost to creating interfaces between the two phases. If the energy cost of creating an interface is large, or if the transition is *cooperative*, we expect to see a *grain-boundary growth* dominated transition. If there is just one site where the phase transition can occur, then the rate equation can be written as:

$$\frac{dn_f}{dt} = -k_u + k_f, \quad (82)$$

where  $k_u$  is the rate of unfolding and  $k_f$  is the rate of folding. We assume that there exists a transition state between the two phases whose force- and temperature-dependent free energy per unit reference length is  $g^*(f, T)$ . Then, from Arrhenius-type kinetics, we know that

$$k_u = \alpha_0 \exp \left[ -\frac{l_u \left( g^* - r \left( k_B T \sqrt{f/K_f - f} \right) \right)}{k_B T} \right], \quad (83)$$

and

$$k_f = \beta_0 \exp \left[ -\frac{l_u \left( g^* - (W_B + k_B T \sqrt{f/K_{bu} - f}) \right)}{k_B T} \right], \quad (84)$$

where  $l_u$  is the reference length per base-pair. The quantities following  $g^*$  in the exponents in Eqs. (83) and (84) are nothing but the free energies of the two phases (see also Eq. (30)). However, for a single interface,  $\dot{x} = L_c dn_f/dt$ , where  $L_c$  is the reference contour length. This allows us to write, for a single interface:

$$\dot{x} = L_c \exp \left[ -\frac{l_u g^*}{k_B T} \right] \left( \beta_0 \exp \left[ \frac{l_u \left( W_B + k_B T \sqrt{f/K_{bu} - f} \right)}{k_B T} \right] - \alpha_0 \exp \left[ \frac{l_u r \left( k_B T \sqrt{f/K_f - f} \right)}{k_B T} \right] \right). \quad (85)$$

At equilibrium in a constant force ensemble,  $\dot{x} = 0$  and Gibbs' free energy per unit reference length of the two phases is equal. But the arguments in the exponentials above are exactly the Gibbs free energy per unit reference length in the unfolded and folded phases, respectively. To get zero  $\dot{x}$  when the free energies of the two phases are the same, we expect  $\beta_0 = \alpha_0$ . We can, therefore, absorb this constant into the constants outside and say

$$\dot{x} = M \left( \exp \left[ \frac{l_u \left( W_B + k_B T \sqrt{f/K_{bu} - f} \right)}{k_B T} \right] - \exp \left[ \frac{l_u r \left( k_B T \sqrt{f/K_f - f} \right)}{k_B T} \right] \right), \quad (86)$$

where  $M$  is some constant. This resembles the form given by Abeyaratne and Knowles (2006). Now, the free energy per unit reference length is given by (53). Thus,

$$\dot{x} = M \left( \exp \left[ \frac{l_u \left( W_B + W(\lambda_u) - f \lambda_u \right)}{k_B T} \right] - \exp \left[ \frac{l_u \left( W(\lambda_f) - f \lambda_f \right)}{k_B T} \right] \right). \quad (87)$$

If we now make the approximation  $e^x = 1 + x + O(x^2)$ , assuming that the arguments of the exponentials are small,

$$\dot{x} = M \frac{l_u}{k_B T} (|W| - f_x[|\lambda|]), \quad (88)$$

which shows that in this limit, the phase boundary speed is a function of the driving force alone. Later in this paper, we have used a linear kinetic relation like the one above for reproducing sawtooth patterns in force-extension curves. This kind of relation is also the starting point for the Abeyaratne–Chu–James analysis (Abeyaratne and Knowles, 2006).

Grosberg and Khokhlov have used the conventional Ising model (which is an equilibrium theory) to describe the influence of cooperativity on such transitions (Grosberg and Khokhlov, 2002). In its simplest form, the theory has two parameters, which are

$$k_s = \exp \left( \frac{\Delta G(f)}{k_B T} \right) \quad \text{and} \quad \sigma = \exp \left( \frac{-2\Delta G_s}{k_B T} \right), \quad (89)$$

where  $k_s$  is the equilibrium constant for the helix-to-coil transition, and  $\sigma$  is the cooperativity parameter, determined by the extra free energy of the two coil boundaries flanking the helical region,  $2\Delta G_s$ . We now show that the Grosberg–Khokhlov equations reduce to the Arrhenius rate law equation in the limit  $\Delta G_s \rightarrow 0$ , or  $\sigma \rightarrow 1$ .  $\Delta G_s \rightarrow 0$  implies that the

energy penalty to forming interfaces is negligibly small. This should lead us to the conclusion that in such a situation, the unfolding is nucleation-dominated. According to Grosberg and Khokhlov, the fraction of the molecule in the helical (folded) state is given by

$$n_f = \frac{1}{2} + \frac{(k_s - 1)}{2\sqrt{(k_s - 1)^2 + 4k_s\sigma}}. \quad (90)$$

Here,  $\sigma = 1$ , and hence,

$$n_f = \frac{1}{2} \left( 1 + \frac{k_s - 1}{k_s + 1} \right) = \frac{k_s}{k_s + 1}. \quad (91)$$

This implies that

$$k_s = \frac{n_f}{1 - n_f} = \frac{n_f}{n_u}. \quad (92)$$

From the definition of  $s$ ,  $k_f$  and  $k_u$ , we can rewrite the above as

$$k_s = \frac{k_f}{k_u} = \frac{n_f}{n_u}, \quad (93)$$

which is what we arrive at when we consider (81) in equilibrium,  $dn_f/dt = 0$ . On the other hand, when  $\Delta G_s$  is large, the transition is grain boundary-growth-dominated. Therefore, our description is consistent with a generalized helix-coil transition, but we go beyond equilibrium.

### 7.1.1. Results

The Arrhenius kinetic relation produces very interesting behavior. To fully appreciate the numerical calculations, it is essential to look at the variation of the driving force as a function of the force. As shown in Fig. 13, the driving force changes sign at 63.3 pN for the DNA parameters chosen in this paper. This number will obviously change for any other combination of physical constants. However, for DNA, we see that when a zero pulling velocity or constant displacement condition is applied at both ends, the force tends to be 63.3 pN, regardless of whether the nucleation force is above or below 63.3 pN (see Fig. 14). This is a very interesting result because it showcases a kinetic relation that puts the thermodynamic driving force at the center of the force-extension response. It has been shown that the plateau force can be varied by changing the solution conditions, so the change of the 65 pN transition force to 55 and 75 pN is within limits of experiment. This result may be explained by reasoning that in the absence of any external factor that motivates interface motion, the interface would try to achieve a state of equilibrium.

As mentioned above, the criterion  $f_{driv} = 0$  demarcates two types of behavior observed with zero pulling velocity. If the nucleation force is below 63.3 pN (55 pN in Fig. 14), the sign of  $f_{driv}$  requires that the interface should move further outward from the nucleation point at the end of the molecule. This is obviously impossible, and so after nucleation, the

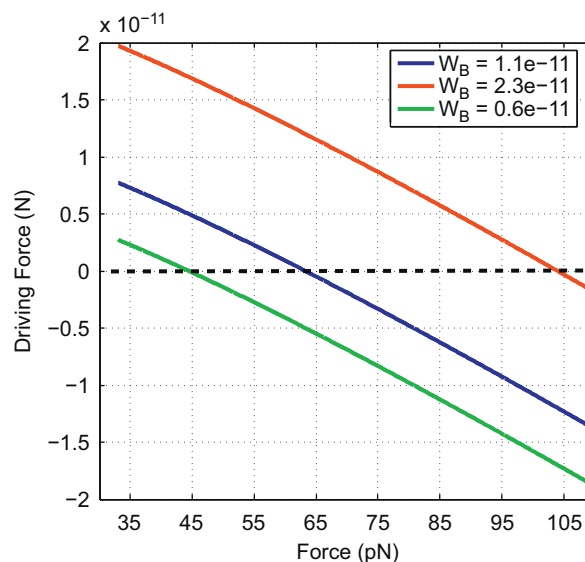


**Fig. 13.** Thermodynamic Driving Force as a function of the force at the interface for DNA parameters. This figure is meant to illustrate the range of  $W_B$  values that cover the range of experimentally observed overstretching forces, approximately 45–105 pN. These are the forces at which the curves cross the  $f_{driv} = 0$  line.

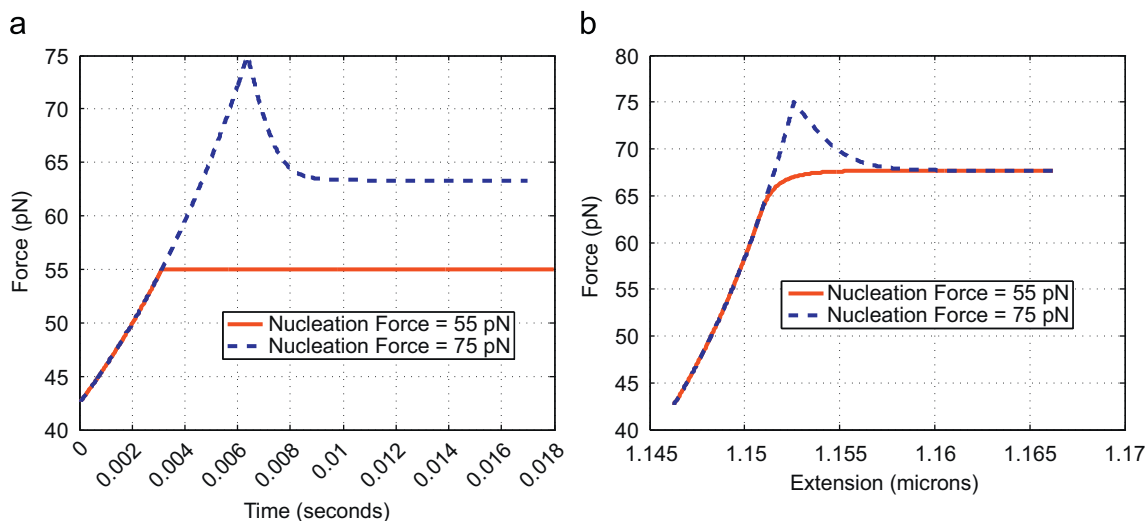


**Fig. 14.** Variation of the force with time in the Arrhenius-type kinetics with  $M=0.005$  and (a) zero pulling velocity, and (b) non-zero pulling velocity ( $1 \mu/s$ ).

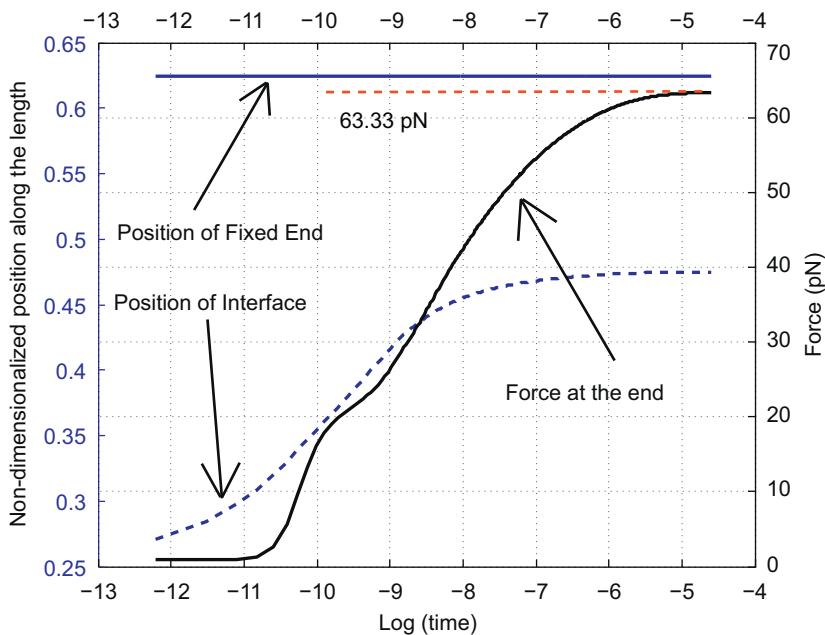


**Fig. 15.** Variation of the force in a partially unfolded molecule with time in the Arrhenius-type kinetics with  $M=0.005$  and zero pulling velocity (black curve). Also shown are plots of the position of the end (fixed) and the position of the moving interface, both in blue. It can be clearly seen that as the interface reaches an equilibrium position, the force also reaches 63.3 pN. Time elapsed is plotted on a log scale. (For interpretation of the references to color in this figure legend, the reader is referred to the web version of this article.)

interface stays stationary and there is no change in the system whatsoever. If the nucleation force is above 63.3 pN (75 pN in the example shown), then the driving force has switched signs, and the interface is required to move along the length of the molecule to begin with. However, this is merely transient behavior. The speed decays shortly after initiation and eventually becomes zero (Fig. 15). The condition for the speed to become zero is when the force in the molecule becomes 63.3 pN, or when driving force becomes zero. This is illustrated in Fig. 14. For the sub-63.3 pN case, we did an additional exercise to show that the force approaches 63.3 pN from below, if allowed to. We assumed as the initial state, a partially unfolded molecule, such as the one shown in the schematic diagram, Fig. 8. Now, while keeping the position of the interface fixed, the molecule was converted to a non-equilibrium configuration by reducing strains on either side. This molecule was then allowed to evolve under a zero pulling velocity, and fixed ends. As shown in Fig. 15, the force rises as the interface moves to increase the force, such that it tends to 63.3 pN. This is essentially a demonstration of the spontaneous re-zipping of a partially unfolded molecule in quasistatic conditions.

In the presence of a finite pulling velocity ( $1 \mu\text{m/s}$  in this case), there are several differences. Since the molecule is continuously being pulled, the force is not expected to stay at the nucleation force if nucleated below the  $f_{\text{driv}} = 0$  line. This is what happens, and the red curve continues to rise, post-nucleation, before it levels out at a force of around  $67 \text{ pN}$ . For the same pulling velocity, if the nucleation occurs above  $63.3 \text{ pN}$ , behavior that is qualitatively similar to the  $v_p = 0$  case is seen. The difference is that instead of settling to  $63.3 \text{ pN}$ , the force becomes constant at the same force as seen for the case in which the transition began at  $55 \text{ pN}$ . Thus, there is a clear tendency for non-zero pulling velocity to push the plateau up.

Since the force in the molecule is not  $63.3 \text{ pN}$ , it is obvious that the driving force is also non-zero. Thus, we expect to see non-zero interface speeds in both these cases. That is also observed (Fig. 16), and as expected, both the red and the blue curves converge to the same non-zero interface speed, which is the reason that we observe a force plateau. It is noteworthy that this system chooses by itself the combination of interface speed and pulling velocity to create a force plateau, without the need to specify it, as we did in the case of a constant interface speed. The kinetic relation is clearly the central character in this cast of variables.

We have also studied the variation of the plateau force as the pulling velocity is changed keeping all other variables the same. We have observed that the variation can be approximated by an expression of the form  $f = a \ln(v_0 - v_p) + b$ , as shown in Fig. 17. A similar result has also been reported by Bertaud et al. (2010) for alpha-helical proteins, on the basis of mesoscale molecular dynamics simulations. The correspondence of this result is further evidence that the model captures features of this problem very well.

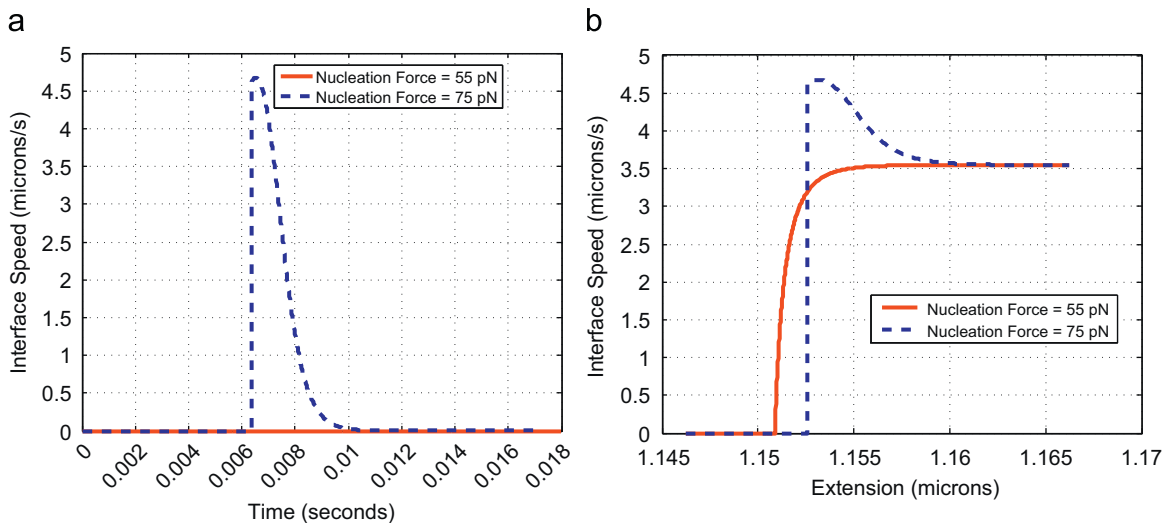


**Fig. 16.** Variation of the interface speed with time in the Arrhenius-type Kinetics with  $M=0.005$  and (a) zero pulling velocity, and (b) non-zero pulling velocity ( $1 \mu\text{m/s}$ ).

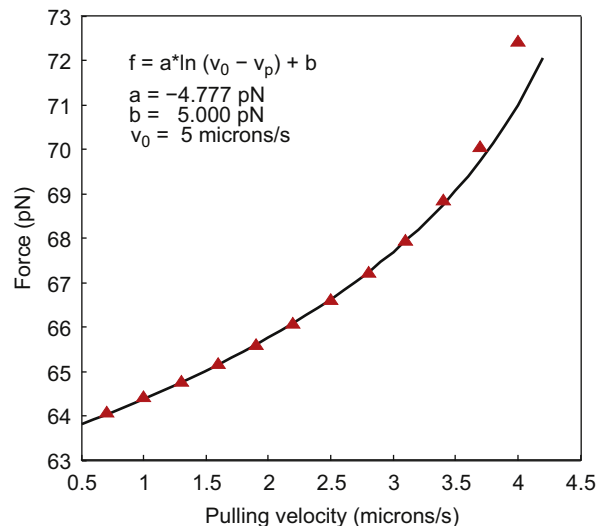


**Fig. 17.** Variation of the plateau force with pulling velocity, and comparison with a logarithmic fit of the form  $f = a \ln(v_0 - v_p) + b$ .

We have also observed the decay of the interface speed to zero as the pulling velocity is increased beyond a limit. Numerically, this is explained by the convergence of the two exponential terms in the kinetic relation to a common value, which causes the interface speed to tend to zero. A closer examination of the factors at work in this regime is quite illuminating. We note that the Arrhenius form chosen for the kinetic relation, and hence for the interface speed, causes the magnitude of the speed to attain a maximum. This is obviously independent of the pulling velocity, and the exact value of this maximum interface speed depends on the parameters  $M$  and  $W_B$ . The dissipation inequality (67) also constrains the thermodynamic driving force and the interface speed to be similarly signed for physical motion of the interface to take place. It is easy to show that the small magnitude of the arguments of the exponential terms effectively reduce it to a linear form in the thermodynamic driving force. The important outcome of this is that both the interface speed and the driving force  $f_{driv}$  are zero at the same value of force. At this point, the interface speed  $\dot{x}$  begins increasing in magnitude from zero.

Owing to the presence of a maximum, the magnitude of  $\dot{x}$  cannot increase indefinitely. As we have seen earlier in this paper, if the pulling velocity  $v_p$  and  $\dot{x}$  reach steady values that lead to a plateau in the force–extension curve, such a steady state is stable and continues till unfolding has completed. However, if  $\dot{x}$  is unable to reach the steady state magnitude for a given  $v_p$  (as given by (76)), then the force continues to rise. Therefore, we have an upper bound on the plateau force that can be achieved. This maximum plateau force clearly corresponds to the ratio  $\dot{x}_{max}/v_p$  through (76). We can find this force,  $f_{plateau,max}$  by equating  $d\dot{x}/df$  to zero. This equation is not explicitly solvable, but a graphical solution is conveniently found.

These calculations can be carried out for any combination of  $W_B$  and  $M$ .  $M$  is simply a scaling factor. It scales the value of  $\dot{x}_{max}$  and has no effect on the value of  $f_{plateau,max}$ .  $W_B$  is more intricately enmeshed in the picture since it also changes the force at which  $f_{driv}=0$ . Therefore, we keep  $M$  fixed for now, and vary the value of  $W_B$ . From this exercise, we extract two quantities for each  $W_B$ :  $\dot{x}_{max}$  and  $f_{plateau,max}$ . As discussed above, we can extract  $(\dot{x}/v_p)_{plateau,min}$  from  $f_{plateau,max}$ . Now, clearly, if the ratio  $\dot{x}_{max}/v_p$  in the experiment being considered is greater than  $(\dot{x}/v_p)_{plateau,min}$ , a plateau will be formed. It is to be noted that the plateau will not always be formed at  $f_{plateau,max}$ .  $f_{plateau,max}$  only tells us the maximum plateau force achievable with the system parameters. Also, it is worth noting that  $\dot{x}_{max}$  alone does not determine whether a plateau will be formed or not. For the same  $\dot{x}_{max}$ , a small  $v_p$  will allow attainment of steady state, but a larger value may not. Therefore, to summarize, the condition for a plateau to be formed is

$$\frac{\dot{x}_{max}}{v_p} \geq \left(\frac{\dot{x}}{v_p}\right)_{plateau,min} \quad (94)$$

This result has been shown in Fig. 18. Now, we can see how changing the value of  $M$  can influence whether a plateau is formed or not. Increasing  $M$  pushes a greater part of the curve above the plateau threshold, equivalent to decreasing  $v_p$ . Physically, it is our opinion that this non-plateau region denotes a nucleation-dominated regime for phase transitions that might come into effect at higher pulling velocities. Since our computation assumes the existence of only one interface, the phase diagram in Fig. 18 suggests that at higher pulling velocities, a picture with only one phase boundary becomes untenable, and other interfaces must be nucleated to propagate the unfolding along the length of the molecule. At each of these nucleation sites, the above kinetics may be applied. Thus, our model offers a reasoning for the experimental

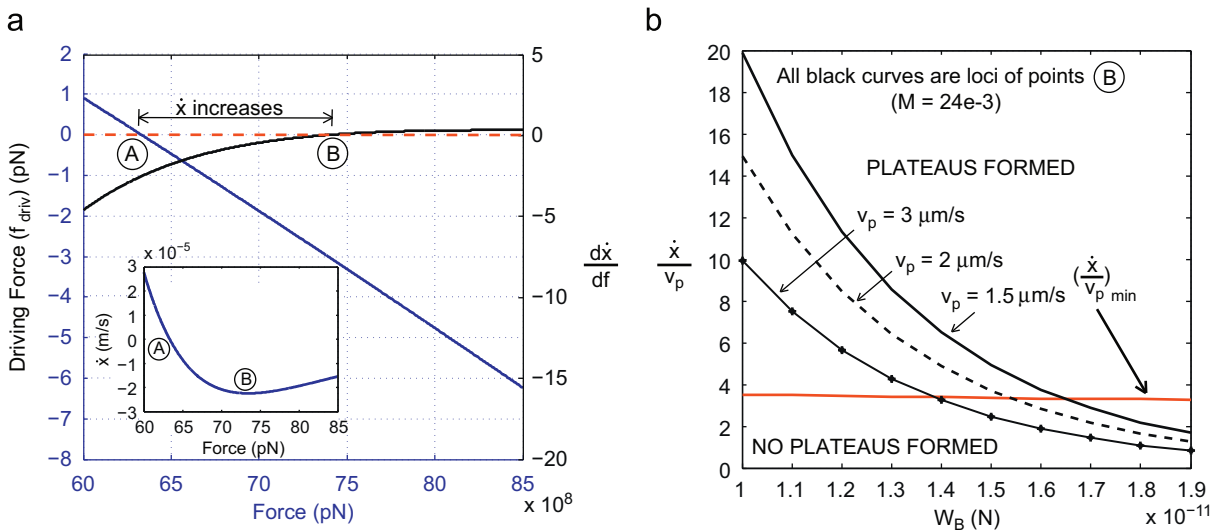


**Fig. 18.** (a) Interface speed  $\dot{x}$  increases in the force range shown.  $d\dot{x}/df$  becomes zero at B, and interface motion begins at A. Inset: Variation of  $\dot{x}$  with force  $f$ . Points A and B are marked. (b) Scaled  $\dot{x}_{max}$  curves are shown in black. These curves can also be understood as loci of points A for different  $W_B$ . The red curve is the  $(\dot{x}/v_p)_{plateau,min}$  obtained from  $f_{plateau,max}$ . (For interpretation of the references to color in this figure legend, the reader is referred to the web version of this article.)

observations that single and multiple interfaces may be seen, depending on the rate of the process. In the next section, we discuss such a process where multiple nucleation events are modeled.

## 7.2. Serrated force-extension curves

This discussion leads us to another class of observed force-extension behaviors, the serrated extension curve. In this behavior, the force does not increase or decrease monotonically, but rather as a sequence of rises and falls. Such a response is seen in molecules which are pronouncedly heterogeneous along their lengths (Fig. 19). Fibrinogen is such a molecule, which is composed of a number of domains joined together by linking elements (Brown et al., 2009). These domains unfold in a violent and fast manner, after the applied force has reached a threshold. After one domain unfolds, the force in the molecule drops due to the sudden increase in length. The force then rises again, until the next domain unravels. The peaks in the force-extension curve are also termed as sawteeth. We will now attempt to recreate the serrated force-extension behavior in a phenomenological way. We assume that the sawteeth arise from a sequence of individual nucleation events, that have approximately the same nucleation criteria. It is different from interface propagation in the absence of significant cooperativity. Transitions with high cooperativity are characterized by a high energy penalty to the formation of new interfaces. This causes an interface, once formed, to propagate along the molecule. If the energy cost for creation of a new interface is small, it is more feasible for unfolding to occur via a sequence of nucleation events, as opposed to a single or very small number of interfaces. In this sense, it is a natural mechanism to discuss, following the Arrhenius-type kinetics, which has shown the possibility of unfolding proceeding via a sequence of nucleation events.

We start with the following assumptions:

1. All sawteeth are between two pre-determined forces,  $f_L$  and  $f_U$ , thus having a fixed amplitude.
2. The rising parts of the plot correspond to zero interface speed, and the falling parts to non-zero interface speed.
3. The second law of thermodynamics must be satisfied unconditionally in the region of the  $f_{driv}-\dot{x}$  plane that is inhabited by the system.

We start by identifying the part of the  $f_{driv}-\dot{x}$  space that is being considered.

This is important because we are trying to model a system in which the phase boundary travels only in one direction, similar to the plateau-like system. Thus, for the second law of thermodynamics to be satisfied unconditionally, the driving force should also have the same sign throughout the unfolding process. Hence, our region of interest in this plot is below the  $f_{driv} = 0$  line. As mentioned above, the falling parts of the force-extension curve correspond to non-zero interface speed. We assume further, that in this regime, the kinetic relation is linear, i.e. the interface speed varies linearly with the driving force. Also, owing to the assumption that all sawteeth are bounded by force limits from above and below, we have bounds on the driving force achieved at the interface. From our knowledge of the variation of driving force with force at the interface, we see that as the force at the interface increases, the driving force also increases in magnitude

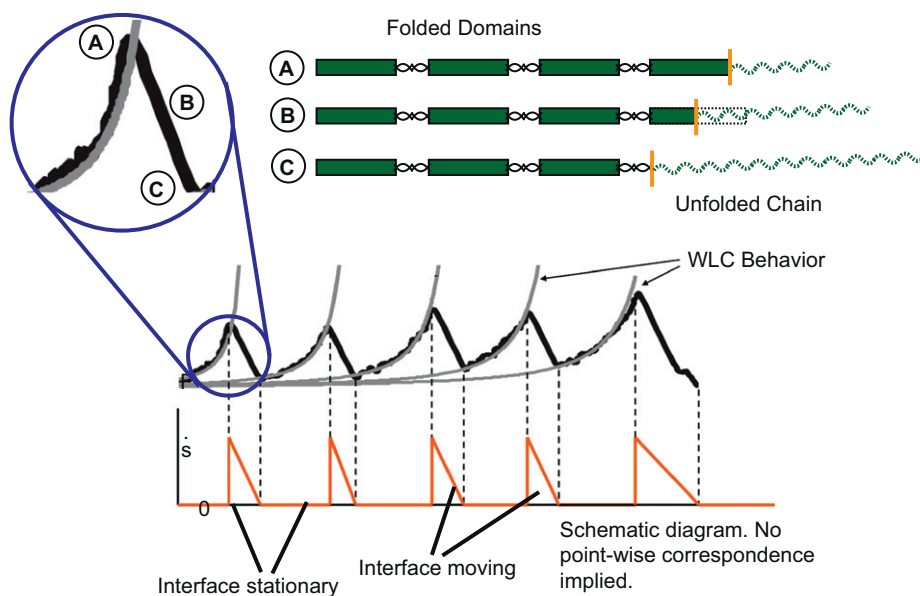
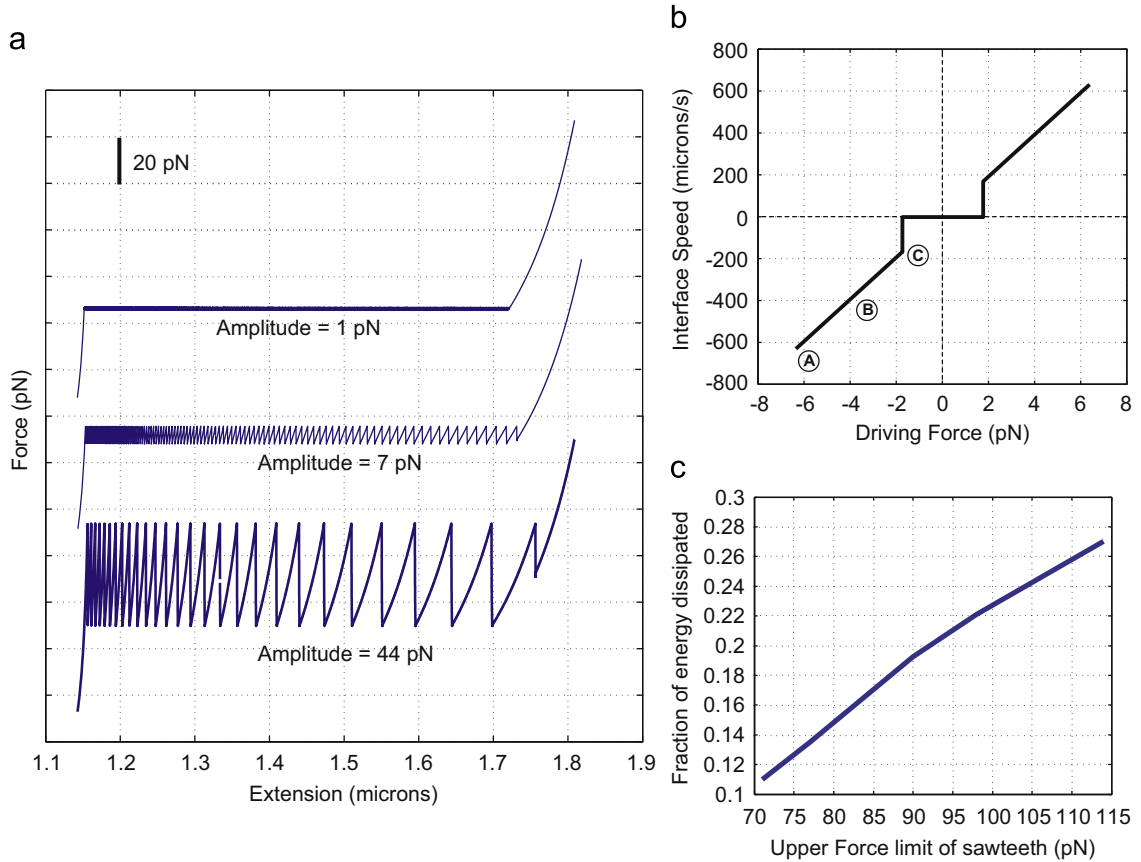


Fig. 19. Schematic diagram showing how alternating zero and non-zero interface speeds create sawteeth (adapted from Lv et al., 2010).



**Fig. 20.** (a) Sawtooth patterns of amplitude 1, 7 and 44 pN generated from linear kinetics. (b) A sample linear sawtooth kinetic relation with the points A, B and C from Fig. 19 shown. (c) Variation of the dissipated energy with the upper limit of sawteeth (lower limit fixed at 70 pN).

(and decreases in value). Thus, the upper force bound for the sawteeth is imposed as a minimum on the driving force (maximum absolute value). Similarly, the lower force bound gives us a maximum (minimum absolute value) on the driving force. Thus the kinetic relation for this case is

$$\dot{s} = \begin{cases} mf_{driv}, & f_{driv,min} \leq |f_{driv}| \leq f_{driv,max} \\ 0 & \text{otherwise,} \end{cases} \quad (95)$$

which is reminiscent of the Abeyaratne–Chu–James analysis for the propagation of a discontinuity through a row of imperfections (Abeyaratne and Knowles, 2006).

We have seen in our study of the plateau-like force-stretch relation that it is possible to get both upward and downward sloping unfolding regions by decreasing or increasing the interface speed (which is a function of the pulling velocity), respectively. In this case, we require that the drop in force be almost vertical, which suggests a very high interface speed. We keep the pulling velocity fixed at 3 μm/s and allow the interface speed to vary in accordance with the chosen kinetic relation. The results are shown in Fig. 20(a). The base of the sawteeth has been kept fixed at 70 pN, while the upper limits are 114, 90, 77 and 71 pN, respectively. In each pattern the sawteeth are more closely spaced at low extensions.

For the pattern in Fig. 20, the amplitude is 1 pN and we can see that it resembles quite closely the plateaus that we have generated earlier. Indeed, it has been suggested that unfolding is not one continuous process, but a number of closely spaced events that produce a nearly horizontal response.

The dissipation rate  $D(t) = f_{driv}\dot{x}$  gives us a method to calculate how much energy is being dissipated in the motion of the interface. In the constant  $\dot{x}$  case, we were able to show that the dissipation is negligible. We expect that because of the intermittent nature of this process, such a conclusion will not be reached here. This was indeed found to be the case, as shown in Fig. 20. The work done on the molecule was calculated by integrating the product  $f v_p$  over time for the entire process, and the dissipation was plotted as a ratio with the work done. We have found that as the amplitude of the sawteeth is increased, more energy is dissipated during the motion of the discontinuity.

## 8. Discussion

In this paper, we have used a theory used to describe phase transitions in continua, and applied it to describe the macromolecule unfolding process under applied force. At the outset, we made contact with the pioneering work of Smith et al. (1996), and showed that our simple one-dimensional framework could reproduce their results on the stretching and relaxation of DNA, thus demonstrating the robustness of the model. We were then able to show that the Abeyaratne–Knowles theory is very effective in providing a robust framework for this description, in spite of the fact that a one-dimensional system such as the macromolecule cannot undergo true phase transitions. We have also shown that with our choice of constitutive law and material constants available in the literature, this system follows the Clausius–Clapeyron equation remarkably well. Not only that, but our value for the latent entropy obtained from this framework is close to previous estimates (Williams et al., 2002). This suggests that if not a true phase transition, it is certainly a plausible and defensible assumption to treat it as such in some scenarios. Of course, the most suggestive feature of the problem, which makes it akin to a first order phase transition, is the presence of a latent heat-like term. Nevertheless, it is noteworthy that we have presented calculations that back up this conjecture.

The propagation of an interface to produce unfolding has recently received endorsement as a mechanism by the groundbreaking experiments of van Mameren et al. (2009). This work, though it was conducted in parallel with that research, employs the same mechanism. We have made several predictions that are within the realm of experimental investigation, with current techniques. The speed of the interface, which had not been hitherto considered, is now an important parameter, and methods being used by researchers today are certainly in a position to further the interplay between theory and experiment on this front. Our work also incorporates considerable flexibility in terms of boundary and initial conditions to be able to replicate a wide variety of experiments. These included stationary and moving fluids, force and displacement boundary conditions, molecules that may be partially unfolded and the ability to accommodate a wide range of macromolecules. With suitable modifications to the constitutive law, the theory has potential to encompass even more polymers.

Our study of different kinetic descriptions also provides a number of grounds of discussion. Firstly, we demonstrated equilibrium and non-equilibrium unfolding processes and also showed that the dissipation in these cases is very different. Up to this point, the quasistatic assumption was quite prominent in approaches to understanding unfolding in polymers. We have derived a number of results and made predictions for such cases. However, we have also shown that with the Abeyaratne–Knowles theory, the rate dependence and non-equilibrium processes are firmly embedded in our model. It is also clear that all three kinetics investigated can produce plateau-like force–extension behavior in appropriate settings. This leads us to realize that these descriptions are limiting cases of one another. The Arrhenius-type description has been shown to reduce to a linear kinetic relation in the limit of small arguments. In the reconstruction of sawtooth-type patterns, we use a linear kinetic relation. In the limit of very small sawtooth height, the resultant behavior is nearly identical to constant interface speed-generated behavior. All three descriptions can, as shown, produce different kinds of responses as well. But the common thread running through them when considering plateau-like behavior is very prominent. In addition, we showed that our model is in line with Grosberg and Khokhlov's results for helix-coil transitions (Grosberg and Khokhlov, 2002), while noting at the same time, that they have unequivocally stated that macromolecule unfolding is not a true phase transition. Thus, our work is compliant with these results as well.

## 9. Conclusion

In this paper, we have considered both equilibrium, and non-equilibrium processes, and shown how a variety of force–extension behaviors in macromolecules may be recreated by appropriate choice of kinetic models for the motion of phase boundaries. The achievement of the model is a comprehensive and rigorous account of how interfaces propagate in macromolecules and the conditions under which such interfaces may or may not be observed. We have also been able to make important connections with a number of available experimental and simulation results that suggest that the model has been successful in describing the process being considered. The most remarkable features of the model is its versatility over several length orders and the introduction of a time scale to a process that has hitherto been studied mainly through the lens of force–extension curves.

## Acknowledgments

We acknowledge partial support for this work from an NSF CAREER award, grant number NSF CMMI-0953548. Mr. Ritwik Raj was partially supported by the Nano/Bio Interface Center at the University of Pennsylvania through grant number NSF NSEC DMR08-32802.

## References

- Abeyaratne, R., Chu, C., James, R.D., 1996. Kinetics of materials with wiggly energies: theory and application to the evolution of twinning microstructures in a Cu–Al–Ni shape memory alloy. *Philos. Mag. A* 73, 457–497.

- Abeyaratne, R., Knowles, J.K., 1990. On the driving traction acting on a surface of strain discontinuity in a continuum. *J. Mech. Phys. Solids* 38 (3), 345–360.
- Abeyaratne, R., Knowles, J.K., 1993. A continuum model of a thermoelastic solid capable of undergoing phase transitions. *J. Mech. Phys. Solids* 41 (3), 541–571.
- Abeyaratne, R., Knowles, J.K., 2006. *Evolution of Phase Transitions: A Continuum Theory*. Cambridge University Press.
- Bertaud, J., Hester, J., Jiminez, D.D., Buehler, M.J., 2010. Energy landscape, structure and rate effects on strength properties of alpha-helical proteins. *J. Phys.: Condensed Matter* 22 (3), 035102.
- Best, R.B., Paci, E., Hummer, G., Dudko, O.K., 2008. Pulling direction as a reaction coordinate for the mechanical unfolding of single molecules. *J. Phys. Chem. B* 112 (19), 5968–5976.
- Brennen, C., Winet, H., 1977. Fluid mechanics of propulsion by cilia and flagella. *Annu. Rev. Fluid Mech.* 9, 339–398.
- Brown, A.E.X., Litvinov, R.I., Discher, D.E., Purohit, P.K., Weisel, J.W., 2009. Multiscale mechanics of fibrin polymer: gel stretching with protein unfolding and loss of water. *Science* 325 (5941), 741–744.
- Chakrabarti, B., Levine, A.J., 2005. Nonlinear elasticity of an  $\alpha$ -helical polypeptide. *Phys. Rev. E* 71 (3), 031905.
- Cluzel, P., Lebrun, A., Heller, C., Lavery, R., Viovy, J.-L., Chatenay, D., Caron, F., 1996. DNA: an extensible molecule. *Science* 271 (5250), 792–794.
- Ericksen, J.L., 1975. Equilibrium of bars. *J. Elasticity* 5 (3–4), 191–201.
- Eshelby, J.D., 1956. Continuum theory of lattice defects. In: Seitz, F., Turnbull, D. (Eds.), *Solid State Physics*, vol. 3. Academic Press, New York.
- Eshelby, J.D., 1970. In: Kanninen, M.F., et al. (Eds.), *Inelastic Behavior of Solids*. McGraw-Hill, New York.
- Grosberg, A.Y., Khokhlov, A.R., 2002. *Statistical Physics of Macromolecules*. American Institute of Physics.
- Kreplak, L., Herrmann, H., Aebi, U., 2008. Tensile properties of single desmin intermediate filaments. *Biophysical Journal* 94 (7), 2790–2799.
- Kulic, I., 2004. *Statistical mechanics of protein complexed and condensed DNA*. Ph.D. Thesis, Johannes-Gutenberg-Universität, Mainz.
- Lv, S., Dudek, D.M., Cao, Y., Balamurali, M.M., Gosline, J., Li, H., 2010. Designed biomaterials to mimic the mechanical properties of muscles. *Nature* 465 (7294), 69–73.
- Marko, J.F., Siggia, E.D., 1995. Stretching DNA. *Macromolecules* 28 (26), 8759–8770.
- Nelson, P.C., 2004. *Biological Physics: Energy, Information, Life*. W.H. Freeman and Company.
- Odijk, T., 1995. Stiff chains and filaments under tension. *Macromolecules* 28(20), 7016–7018.
- Perkins, T.T., Quake, S.R., Smith, D.E., Chu, S., 1994. Relaxation of a single DNA molecule observed by optical microscopy. *Science* 264 (5160), 822–826.
- Purohit, P.K., Bhattacharya, K., 2003. Dynamics of strings made of phase-transforming materials. *J. Mech. Phys. Solids* 51 (3), 393–424.
- Qin, Z., Kreplak, L., Buehler, M.J., 2009. Hierarchical structure controls nanomechanical properties of vimentin intermediate filaments. *PLoS One* 4 (10), e7294.
- Raj, R., Purohit, P.K., 2010. Moving interfaces in rod-like macromolecules. *Europhys. Lett.* 91, 28003.
- Rief, M., Fernandez, J.M., Gaub, H.E., 1998. Elastically coupled two-level systems as a model for biopolymer extensibility. *Phys. Rev. Lett.* 81 (21), 4764–4767.
- Rief, M., Clausen-Schaumann, H., Gaub, H.E., 1999. Sequence-dependent mechanics of single DNA molecules. *Nat. Struct. Biol.* 6 (4), 346–349.
- Rouzina, I., Bloomfield, V.A., 2001. Force-induced melting of the DNA double helix 1. *Thermodynamic Analysis*. *Biophys. J.* 80 (2), 882–893.
- Schwaiger, I., Sattler, C., Hostetter, D.R., Rief, M., 2002. The myosin coiled-coil is a truly elastic protein structure. *Nat. Mater.* 1, 235.
- Smith, S.B., Cui, Y., Bustamante, C., 1996. Overstretching B-DNA: the elastic response of individual double-stranded and single-stranded DNA molecules. *Science* 271 (5250), 795–799.
- Storm, C., Nelson, P.C., 2003. Theory of high-force DNA stretching and overstretching. *Phys. Rev. E* 67 (5), 051906.
- Su, T., Purohit, P.K., 2009. Mechanics of forced unfolding of proteins. *Acta Biomater.* 5 (6), 1855–1863.
- Truskinovsky, L., 1982. Equilibrium phase interfaces. *Sov. Phys. Dokl.* 27, 551–553.
- Truskinovsky, L., 1985. Structure of an isothermal phase jump. *Sov. Phys. Dokl.* 30, 945–948.
- van Mameren, J., Gross, P., Farge, G., Hooijman, P., Modesti, M., Falkenberg, M., Wuite, G.J.L., Peterman, E.W.G., 2009. Unraveling the structure of DNA during overstretching by using multicolor, single-molecule fluorescence imaging. *Proc. Natl. Acad. Sci.* 106 (43), 18231–18236.
- Weiner, J.H., 1983. *Statistical Mechanics of Elasticity*. John Wiley and Sons.
- Williams, M.C., Rouzina, I., Bloomfield, V.A., 2002. Thermodynamics of DNA interactions from single molecule stretching experiments. *Acc. Chem. Res.* 35 (3), 159–166.
- Williams, M.C., Rouzina, I., 2002. Force spectroscopy of single DNA and RNA molecules. *Curr. Opin. Struct. Biol.* 12 (3), 330–336.
- Yanson, I.K., Teplitsky, A.B., Sukhodub, L.F., 1979. Experimental studies of molecular interactions between nitrogen bases of nucleic acids. *Biopolymers* 18 (5), 1149–1170.